RENEWAL REPORT

CaseID: 8488 PermitID: 2821 Sao Jose SHIPWRECKID2658)

Compiled and edited by J Boshoff

iziko
museums of cape town

INTRODUCTION

This is a progress report for the renewal of the permit on the wreck of the slaver *Săo José*. The bulk of the report contains the results from a baseline environmental survey. Due to Covid 19 we were not able to do much fieldwork in the 2019/2020 seasons. We focused on equipment renewal. Funding for the environmental assessment was provided by the US Ambassadors Fund for Cultural Preservation. As this funding is now finished we are busy looking at other funding initiatives. The project employed several external as well as in-house specialists as the different aspects of the study necessitated. We modified the objectives as the project developed and these changes will be discussed where applicable.. The discussion below consists of extracts from various commissioned reports.

The basic structure of the environmental assessment was designed by Dr. Carl Wainmann and adapted by J Boshoff as and where it was felt necessary. Iziko staff was responsible for the field deployment of instrumentation and hereby developed many new useful skills. The Geophysical survey was done under the direction of J. Boshoff with the technical implementation and the interpretation done by the Council of Marine Geoscience. The various specialists were responsible for the interpretation of the other data generated.

WRECK SITE LOCALITY

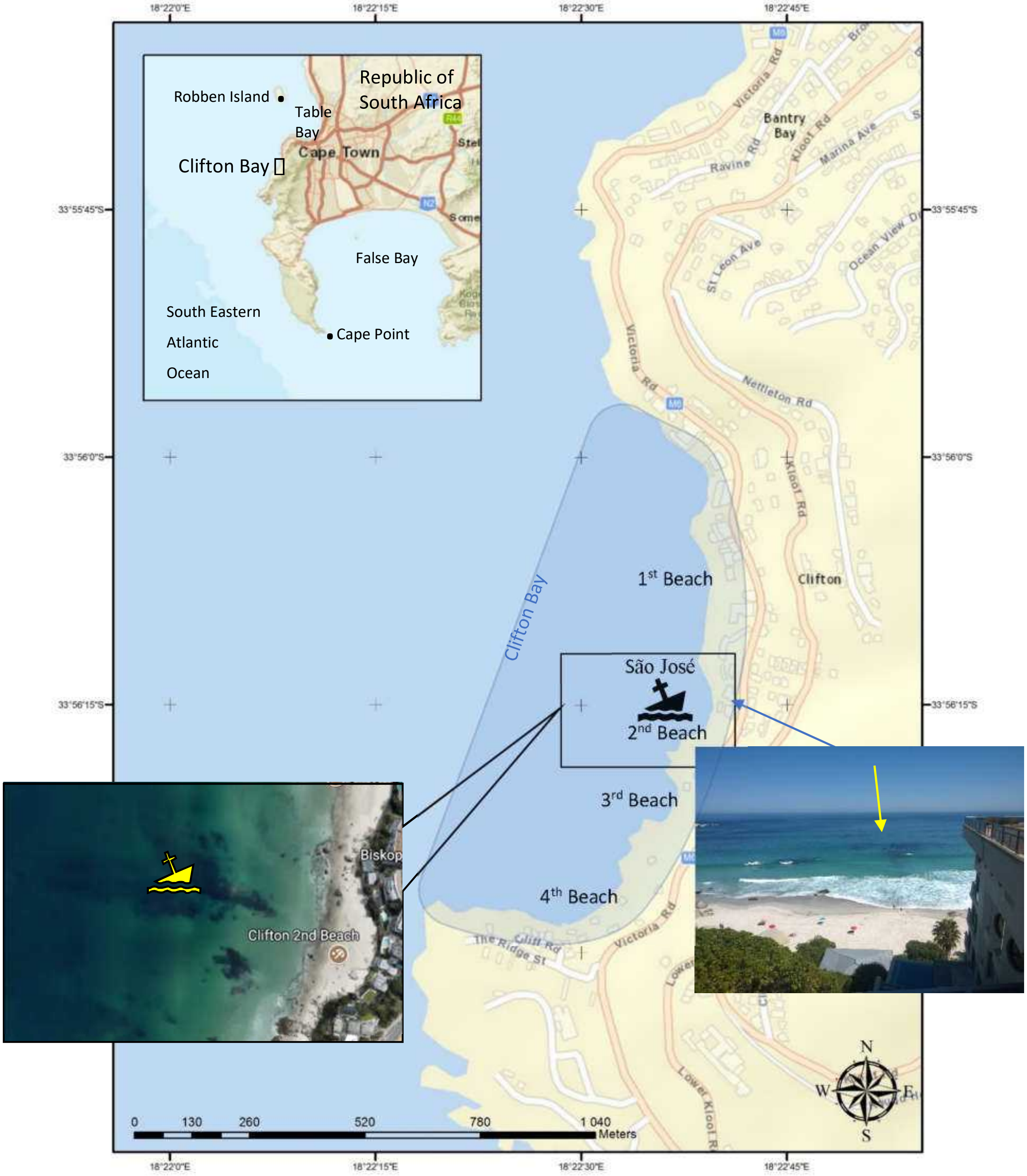

Geographic setting

"*Cape Town is a port city on South Africa's southwest coast, on a peninsula beneath the imposing Table Mountain. Slowly rotating cable cars climb to the mountain's flat top, from which there are sweeping views of the city, the busy harbor and boats heading for Robben Island, the notorious prison that once held Nelson Mandela, which is now a living museum. Clifton Bay is located close to the City of Cape Town metropole with approximately.*" (www.google.co.za, accessed 3/26/2021)

In 2017, the City had a population of 3.74 Million. 2nd Beach Clifton is one of 4 (Clifton 1st, 2nd, 3rd and 4th) popular summertime beach tourist destinations in Cape Town.

The City of Cape Town Beach report of 2009 described the coastal locality as follows: "*This stretch of coastline provides a convenient outdoor escape for people living in the city bowl and neighbouring areas, and also attracts residents of outlying suburbs, as its beaches are the most sheltered in Cape Town. Although the sea is too cold for more than a quick dip, the beaches face the setting sun, making for longer days as well as spectacular sunsets.*"

The adjoining coastal zone consists of mostly high-income holiday accommodation. The area bordering the beach is steep due to its proximity to the Twelve Apostles mountain range which adjoins Table Mountain. Although 4 popular beaches have been named due to their popularity, the greater Clifton Bay (inclusive of all 4 beaches) has an additional un-named small seasonal beach at its northern extent. This is significant in the context of this project since it represents a proxy for beach erosion of the bay. This is due to its perpendicular alignment to the prevailing Atlantic swell.

"*Cape Town's 2017 population is now estimated at 4,709,990. In 1950, the population of Cape Town was 618,000. Cape Town has grown by 92,430 since 2015, which represents a 2.00% annual change. These estimates represent the Urban agglomeration of Cape Town, which typically includes Cape Town's population in addition to adjacent suburban areas.*" (http://worldpopulationreview.com/world-cities/cape-town-population/ accessed 3/26/2021).

Bathymetry

Hydrographic Survey standards demand high integrity of data, undertaken by a certified Hydrographic surveyor. Their purpose is normally maritime based and important since if the ocean depth is not accurately known, there is a risk of vessel damage. In all qualified survey instances these complex datasets and procedures are rigorously tested for compliance to conformance.

Hydrographic quality bathymetric survey standards were however not required for this project. Using a simple approach of maximizing opportunistic data collection from repeated boat visits to the wreck site a ‘programme’ of repeated bathymetric ‘survey’ lines were undertaken. The concept was to use the data collected from a simple single beam fisherman’s echo sounder mounted aboard Iziko museums’ dive tender. This approach also limited the effort spent to the area of interest only yet repeated often enough to detect changes in sediment depth as time progressed for the project. This was also deemed the most important parameter (seafloor dynamics) at the start of the project and allowed us to compare onshore beach dynamics with offshore seafloor sediment dynamics.

MONTHLY INSHORE/OFFSHORE BATHYMETRIC SURVEY RESULTS

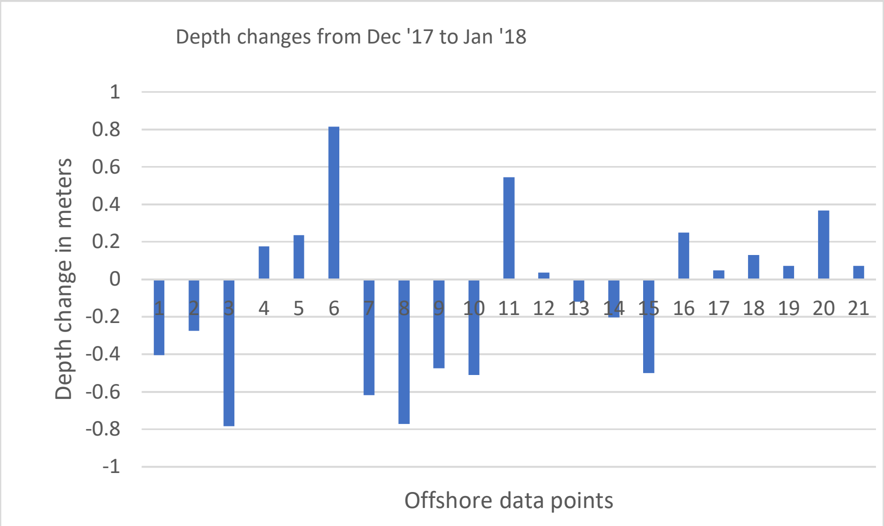

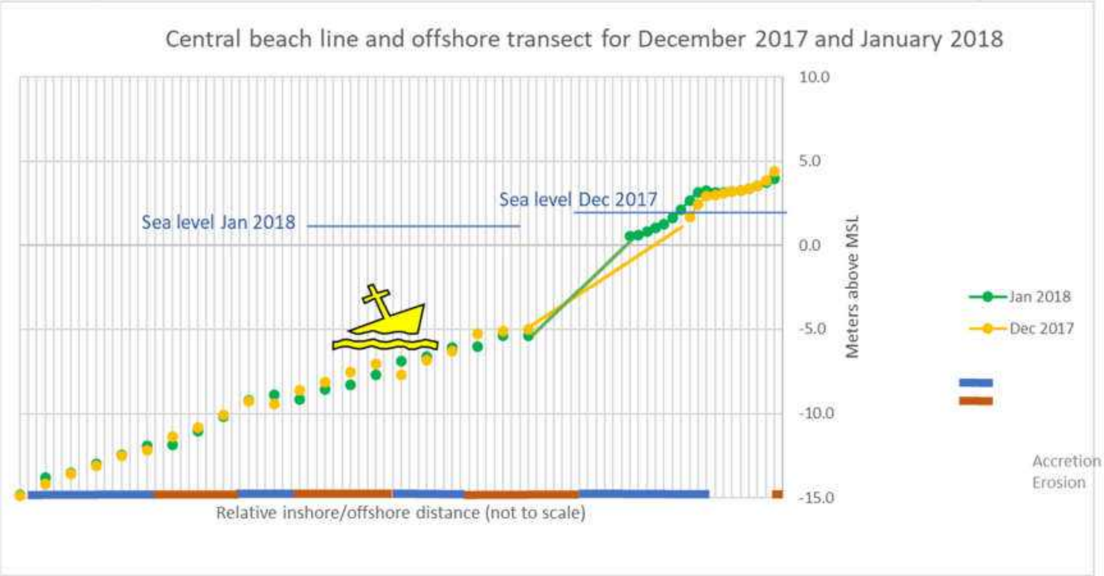

Geomorphology

This section contains extracts from two reports done by the Council for Marine Geoscience and describes the underwater geology and bathymetry of a large part of Clifton bay (Van Zyl, Salzman and Pillay 2018, Van Zyl 2018).

Introduction

IZIKO Museums of South Africa recently contracted the Council for Geoscience to perform high-resolution multibeam bathymetry and single channel, pinger, seismic assessments of the shallow near shore off Clifton Beach in Cape Town, Western Cape. A predefined survey area comprising four areas of varying priority were delimited (See Figure 1 from client). Survey operations took place on the 10th and 12th January 2018. The areas have been referred to as Areas 1 through 4 based on their order of priority. The purpose of the investigation was to obtain clarity on the nature of the seafloor offshore Clifton Beach, where the wreck identified as the *São José-Paquete de Africa* is located with the hope of gaining a better understanding of the sediment dynamics in the region. The seafloor bathymetry, bedrock morphology and elevation, and sediment thickness were assessed.

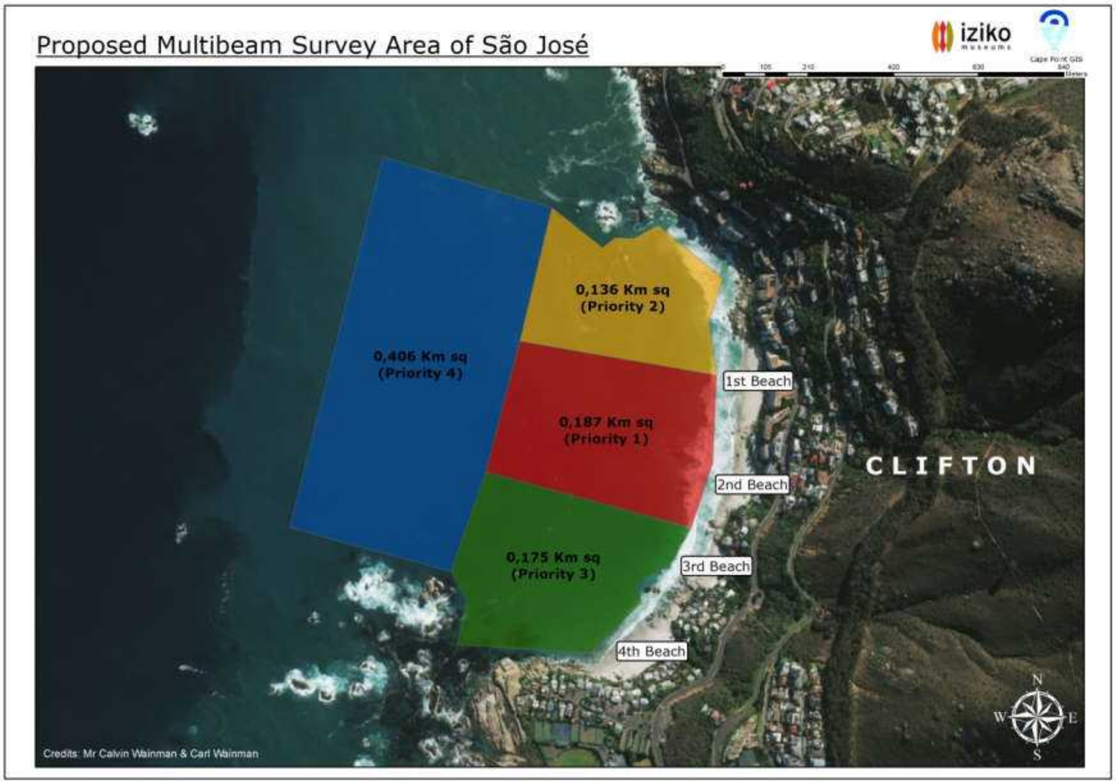

FIGURE 1: Proposed survey area offshore of Clifton Beach. Designated survey areas hereafter referred to as Areas 1, 2, 3 and 4 in order of decreasing priority

Geophysical Survey Methodology

Multibeam echo sounder lines were run roughly parallel to shore and followed previous line trajectories so as to obtain a minimum of 20% overlap between adjacent swaths. Line spacing was determined by the specified overlap, minimum and maximum depths on each path, and predetermined angular beam width settings.

Survey speed was dependent on sea conditions, proximity of obstacles and survey direction and was oftentimes constrained by the vessel’s ability to maintain sufficient swath overlap when steering over rapidly changing terrains (in terms of depth, ruggedness, dip-direction and gradient). It was generally kept below 6 kts.

Pinger Seismic Profiling Survey

Single channel, pinger seismic profiling data were acquired along lines spaced at 20 m intervals running perpendicular to shore in a NNE-SSW orientation (Figure 6). Areas 1, 2, 3 and the majority of Area 4 were covered, however, a shallow outcrop immediately offshore of Second Beach prevented the vessel from safely navigating through this area and this was by necessity omitted.

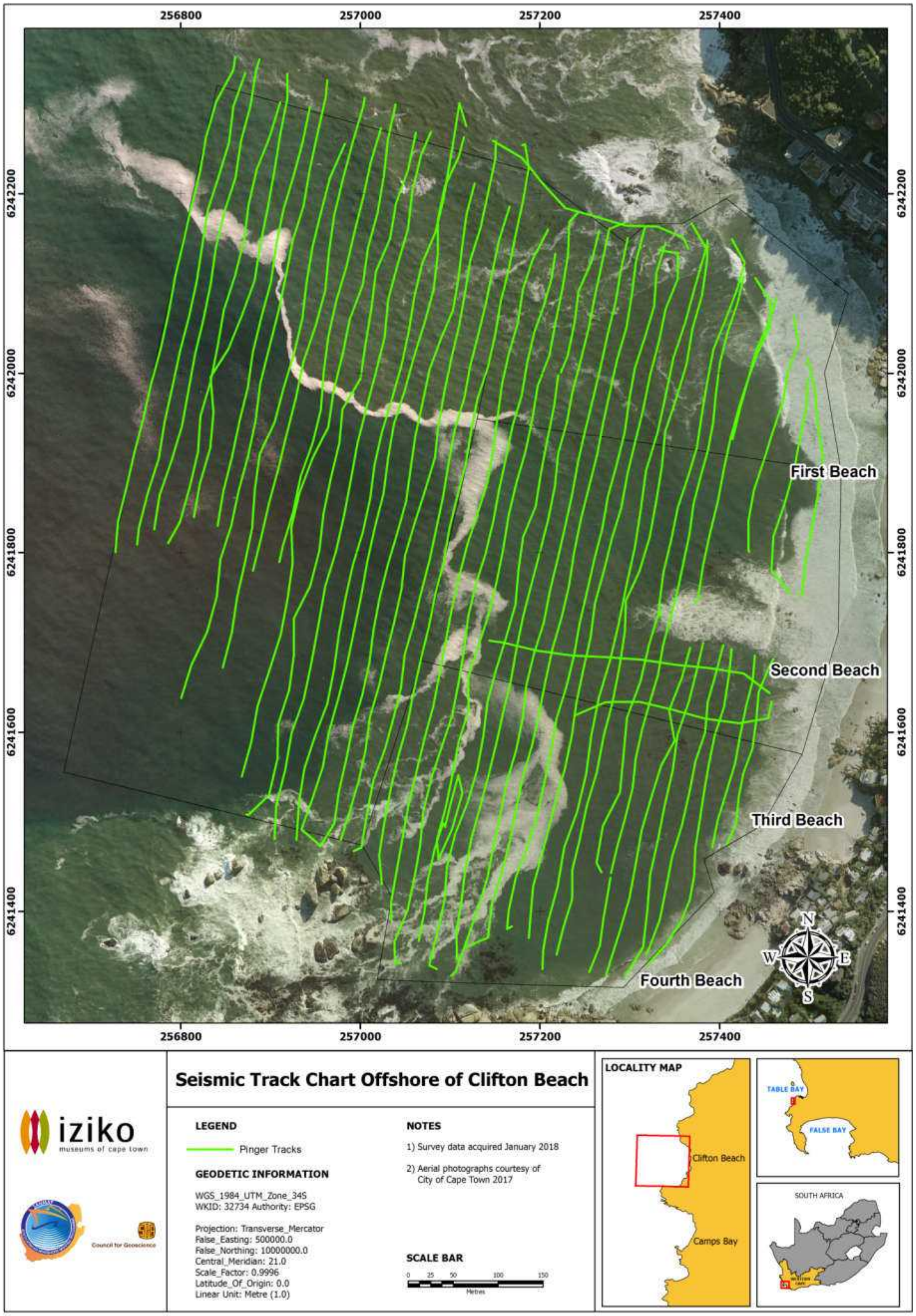

Figure 6: Track chart illustrating lines driven during pinger seismic survey

Multibeam Bathymetry

The multibeam bathymetry data were collected using the WGS84 spheroid and UTM Zone 34 South projection. The SAGEOID2010 orthometric geoid was used as the vertical datum making all seafloor elevations relative to mean sea level (MSL).

Data were acquired as close inshore as was safe to navigate. In some parts of the survey area extremely shallow rock outcrops also prevented data acquisition as these areas were unsafe for vessel access. Apart from this, full coverage with good overlap was obtained within the survey area (Figure 8 & Figure 9).

The acquired bathymetric data extended from 0.5 – 21.4 m below mean sea level (BMSL). The seafloor deepened (at a gradual slope of ~2°) from the shoreline towards the offshore forming a bowl-like depression from the rims of the bay toward the central, offshore portion of the bay. Exceptions occurred in areas where protruding bedrock led to local shallowing.

It is apparent from the multibeam bathymetry that the vast majority of the area comprised either exposed outcrop or shallowly covered bedrock typified by a rugged and high-relief bathymetric expression. The bedrock displays prominent NW-SE, WNW-ESE and ENE-WSW joint sets where bedrock is exposed and gullies tend to be aligned with these (Figure 7). The near shore is dominated by unconsolidated sand. Moving offshore, the sediment cover appears gradually but progressively to thin as water depth increases and wave and tidal action are reduced (Figure 17; Sections 1, 2 & 4). Here bedrock comprises the majority of the seafloor with a highly rugose and bulbous expression on bathymetric imagery. In the center of the embayment, bedrock is almost continually exposed from the shoreline at Second Beach towards the offshore.

In sandy regions of the embayment, sediment bed forms tend to be sparse and subdued. Short-wavelength, shore-perpendicular oscillatory wave ripples are, however, abundant towards the shoreline and where coarser sediments make up the surficial deposits.

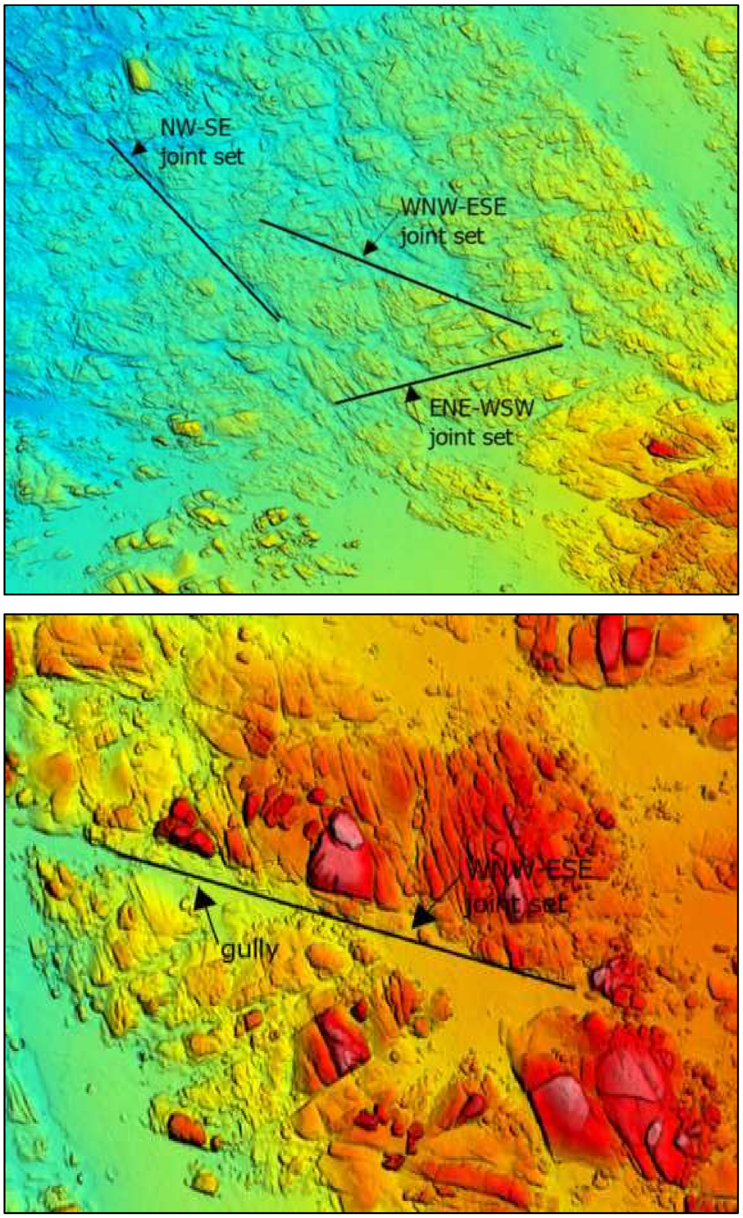

Figure 7: Orientation of joints and discontinuities on the seafloor and the alignment of gullies with these

The inshore, sheltered seafloor of Areas 2 and 3 was almost exclusively comprised of soft sediment with a smooth and flat surface; whereas in Areas 1 and 4 and along the northern border of Area 3 rough, high-relief bedrock exposures dominated.

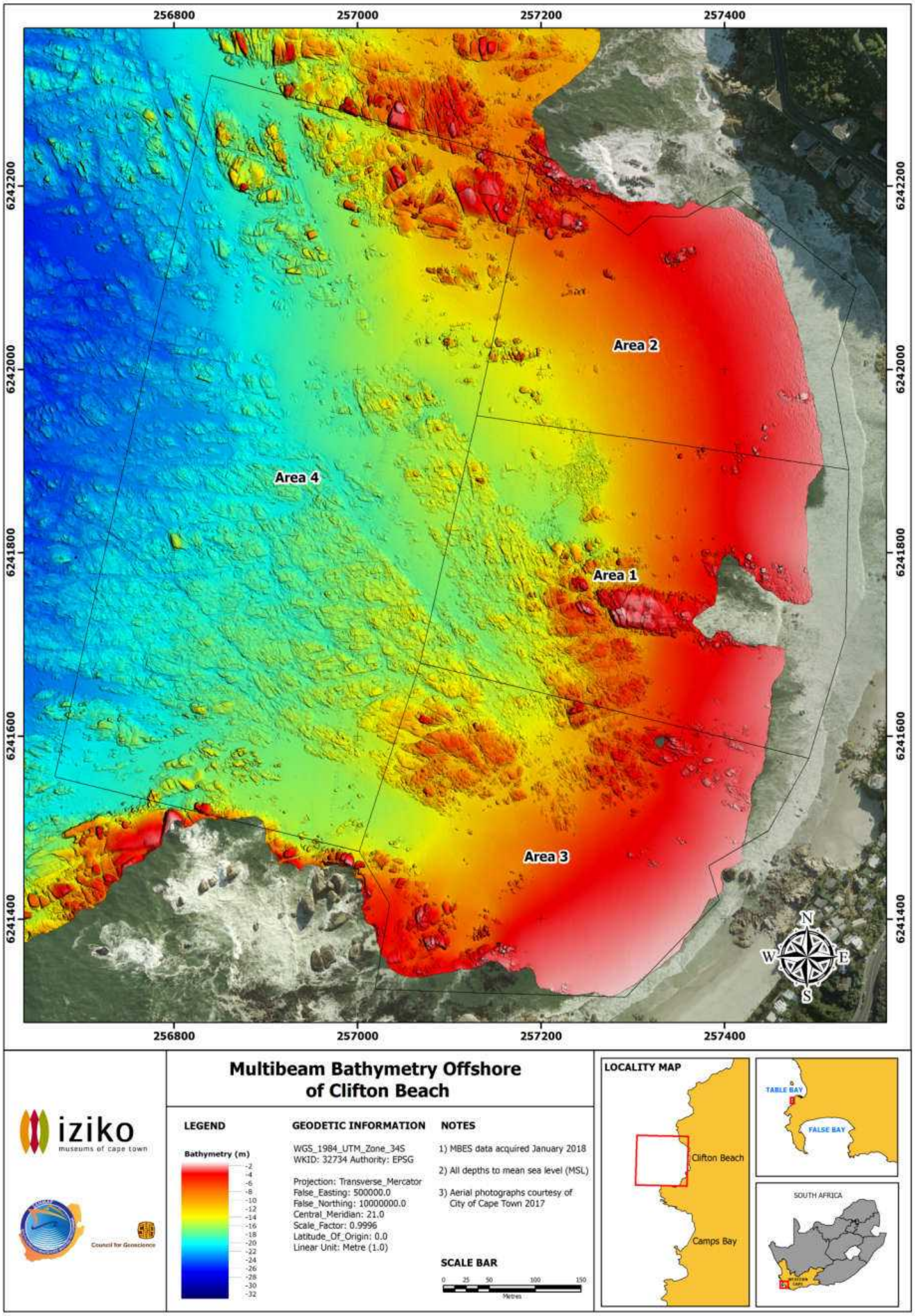

Figure 8: Multibeam bathymetry chart offshore of Clifton Beach

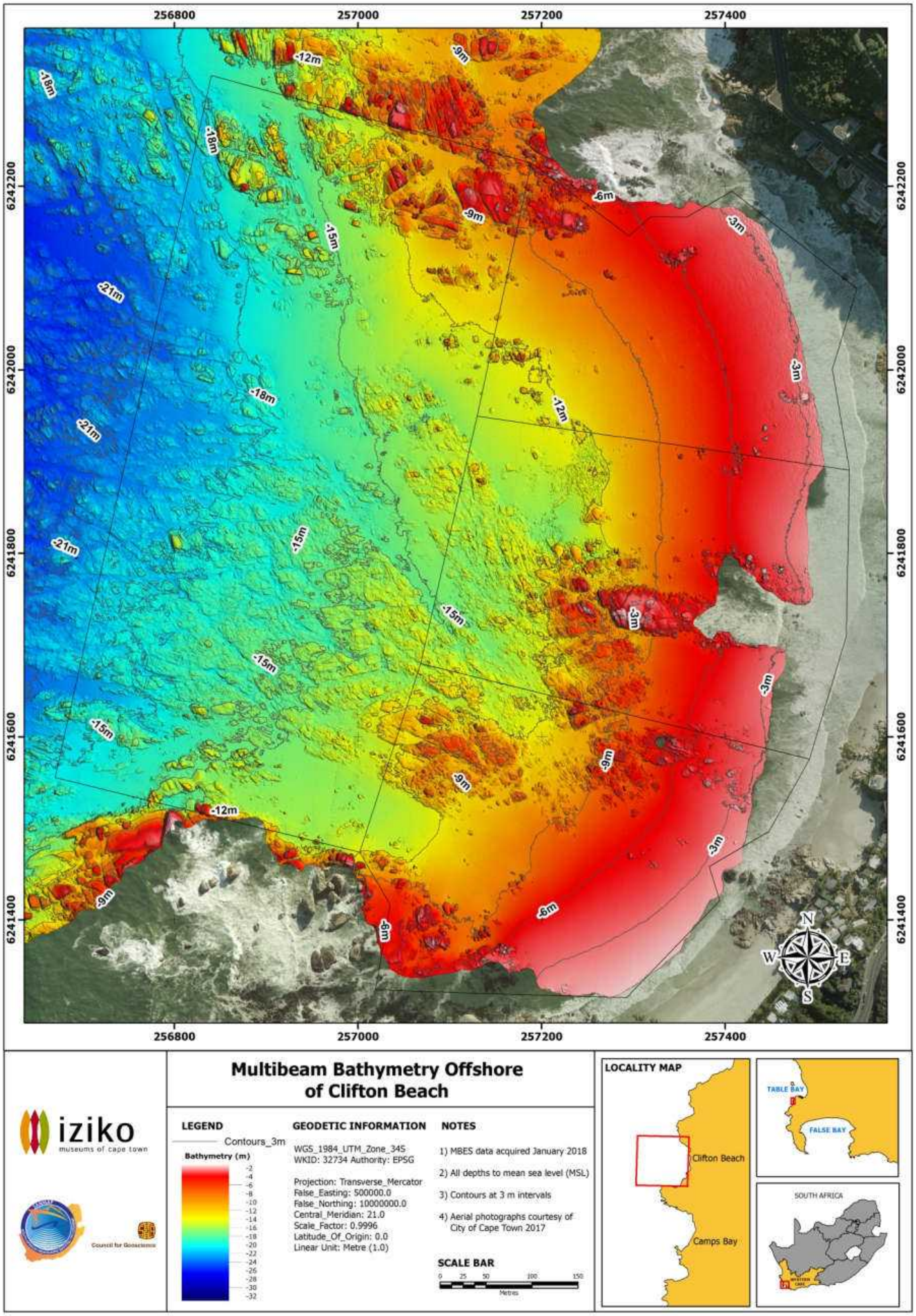

Figure 9: Multibeam bathymetry chart offshore of Clifton Beach showing isobaths (contours) at 3 m intervals

Seafloor Geology

A side scan sonar mosaic was derived from backscatter data collected with the multibeam system. The side scan sonar mosaic presented in Figure 10 depicts the variation in seafloor 'reflectivity' across the survey area. In such side scan sonar mosaics, tone and texture are representative of the nature and geomorphology of the seafloor (Schimel et al., 2015). Under the color scheme used, higher reflectivity seafloor substrates are characterized by darker returns whilst lower reflectivity substrates are displayed as brighter returns. Thus, bedrock is portrayed in backscatter images by dark grey colors, while softer sandy to muddy sediments provide lighter grey returns. The smooth dark grey areas are interpreted as bioclastic gravel or shell. Shell has a harder return than sand, giving a darker return. The high relief and rugosity of bedrock as well as its intensely fractured nature pose a distinct contrast with the flat, featureless surface formed by unconsolidated sediments.

The acoustic (seafloor geology) facies interpretation is shown in Figure 11. The interpretation was done using a combination of the side scan sonar mosaic and the multibeam bathymetry. Five acoustic facies have been identified and correlated with on land geological formations. The various facies, their aerial extent and correlated geological formation are presented in Table 1.

Facies	Aerial Extent	Percent Areal Coverage	Geology
Sand	304,963 m^2	25.4%	Witzand Formation
Bioclastic Gravel	74,520 m^2	6.2 %	Witzand Formation
Boulder Beach	5,058 m^2	0.4 %	Quaternary cover
Scattered Reef	26,862 m^2	2.2 %	Cape Granite
Prominent Reef	790,634 m^2	65.8 %	Cape Granite

Table 1: Seafloor geology facies used with corresponding geology

The dominant facies in the area constitute prominent reef and sand facies. The sand facies is mostly found on the inshore while prominent reef facies are to the offshore. Bioclastic gravels are mostly constrained to in the offshore gullies with some larger areas to the south of the bay. A small area of boulder beach facies was interpreted in Area 1. The texture appears similar to well-rounded large cobbles or small boulders found in other areas which often collect on paleo beaches at lower sea level. Visual inspection will be needed for conclusive identification. An elaboration on each of the identified seafloor facies is provided below.

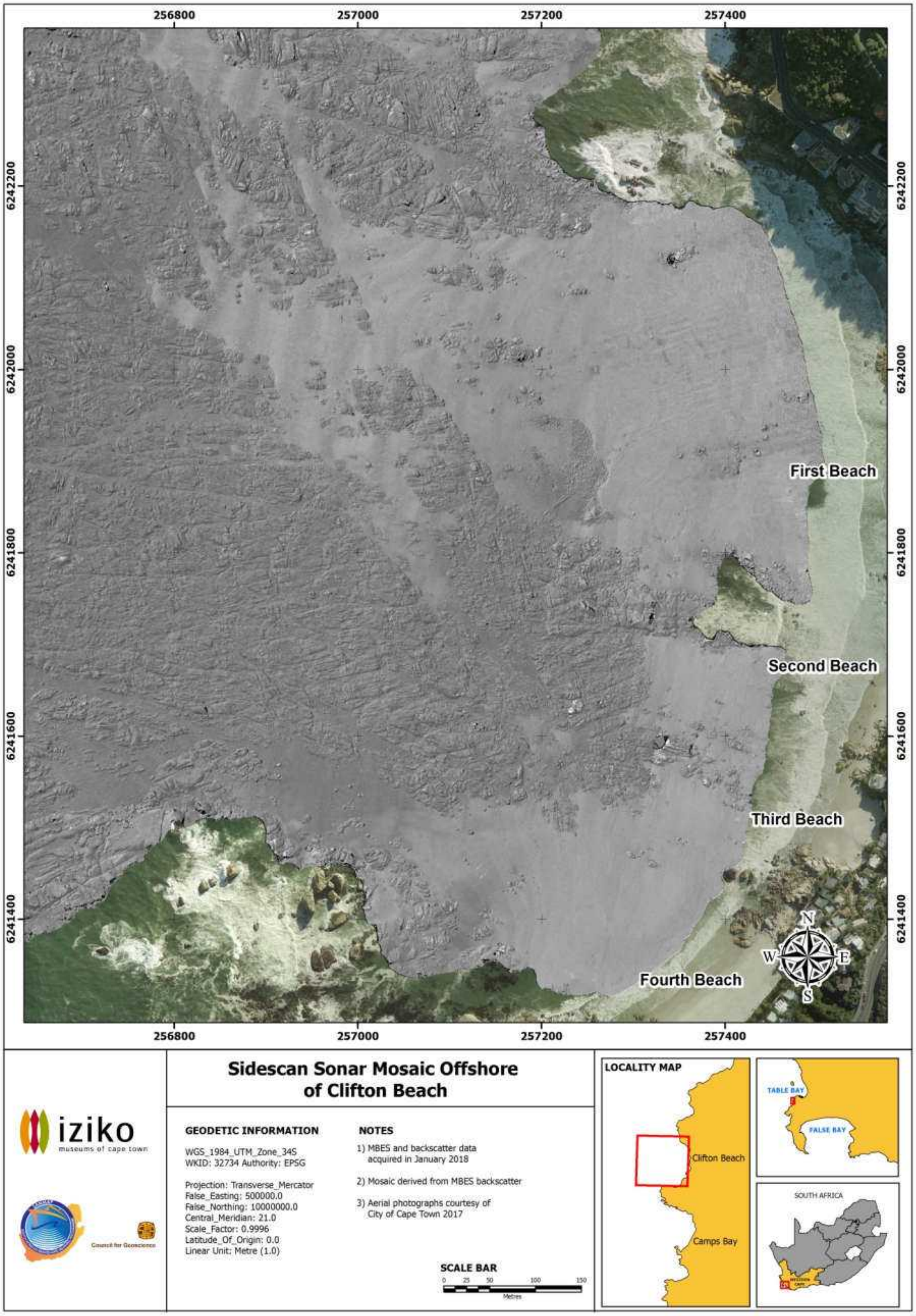

Figure 10: Side scan sonar mosaic obtained using backscatter data from the R2Sonic Multibeam system

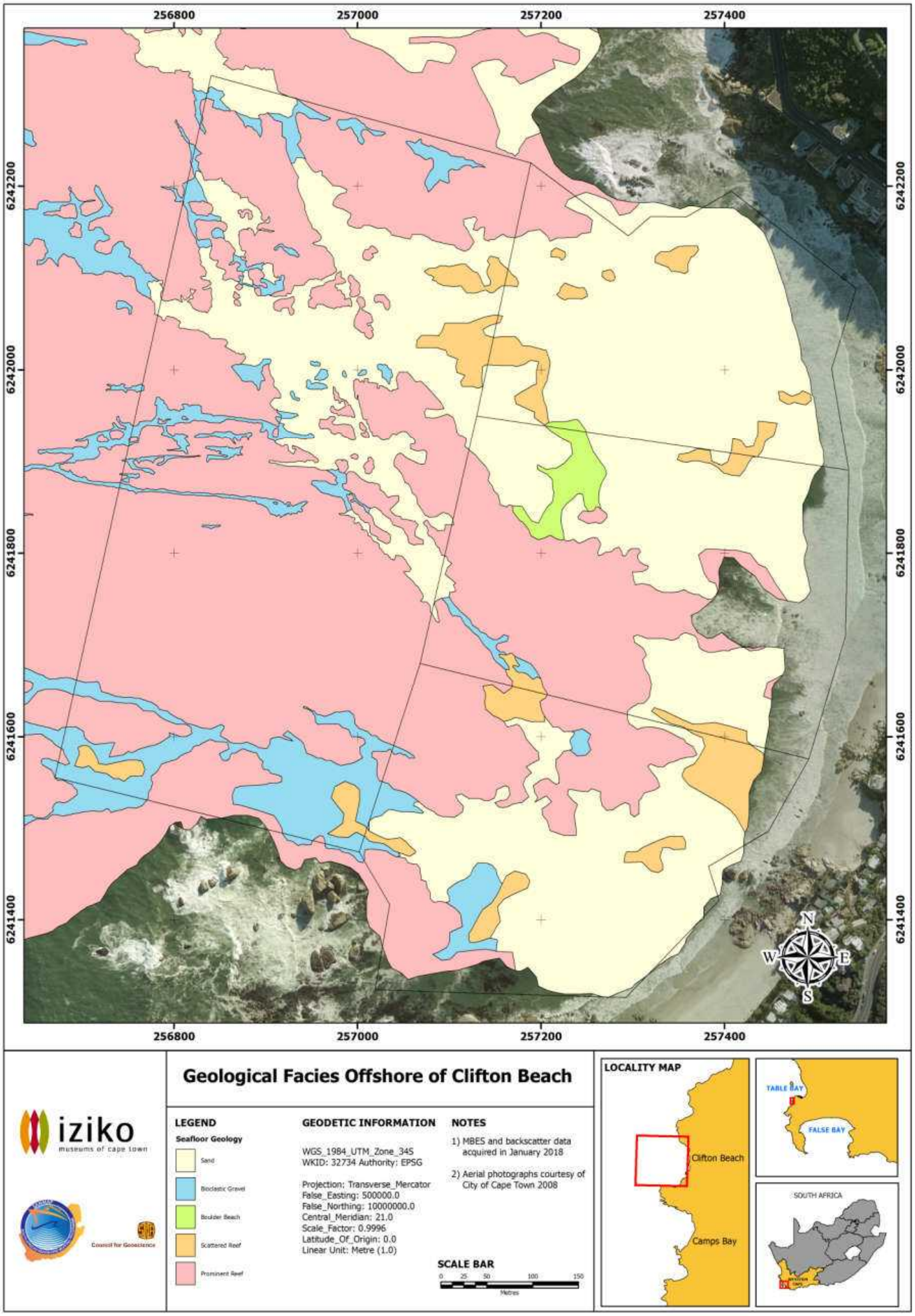

Figure 11: Interpreted acoustic facies for the study area. Section localities are shown for Figure 18

Sand Facies

The sand facies poses light (weak) returns and a smooth, relatively featureless surface on the backscatter mosaic. Ripples become increasingly common toward the high-energy shoreline and where courser lags form seaward of obstructions (Figure 12). The sand facies comprises unconsolidated sand-sized sediment of the Witzand Formation and is the second most abundant facies type, covering 25.4% of the mapped area.

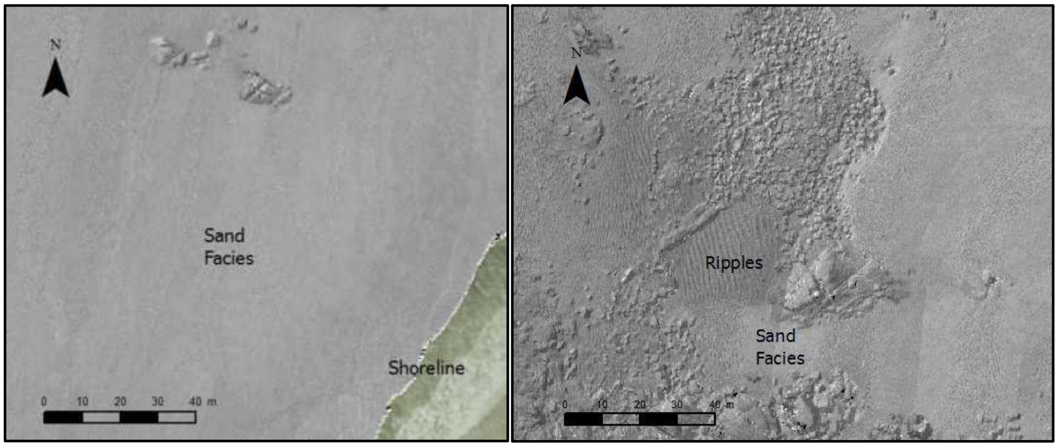

Figure 12. Backscatter mosaic displaying the acoustic signature of the sand facies.

Bioclastic Gravel Facies

The Bioclastic Gravel Facies has a slightly harder (darker) return than the sand facies due to its composition of harder and more reflective material. It has a fairly uniform, grainy acoustic signature (Figure 13), and often displays symmetrical, bifurcating bedforms or wave ripples on the seafloor running perpendicular to wave shoaling direction. From experience sampling this facies in similar areas the authors postulate that this reflective material is mainly composed of dead organic detritus that is shed from reef outcrops in the form of sponge spicules, shell and cirripede fragments and small rock fragments. This coarser material collects in the troughs between bedforms. From the sonographs, the bedforms show varying orientations reflective of the different wave/swell direction vectors which formed them. Within the survey area this facies is the third most dominant accounting for 6.2 % of the total area. The facies occurs predominantly between Reef Outcrop in offshore areas.

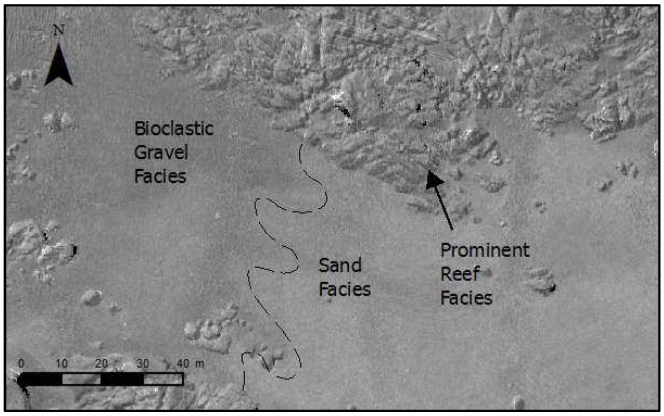

Figure 13: Backscatter mosaic displaying the comparatively harder (darker) returns of the bioclastic gravel facies with the softer (lighter) returns of the sand facies. Note the gradual transition from one facies to the other (dashed line)

Boulder Beach Facies

The boulder beach facies is an anomaly within the surveyed area, forming only 0.4% of the mapped seafloor surface and is, therefore, the least abundant facies. This facies is characterized markedly contrasting returns of varying intensity. Boulders partially embedded in sand sized sediments make up this facies and provide the variable returns seen in backscatter images as well as the high-relief observed in multibeam bathymetric images (Figure 14).

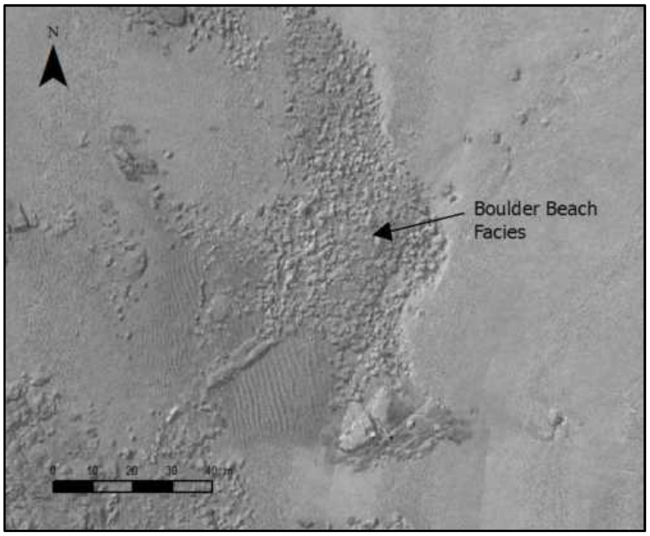

Figure 14: Contrasting return intensities and rounded bedforms characteristic of the boulder beach facie

Scattered Reef Facies

The Scattered Reef Outcrop is directly related to the Prominent Reef described below. The polygons which define this facies consist of zones made up of rock and sand in approximately equal proportions (Figure 15). They typically represent zones where sediment mantles the pre-existing basal rocks with relative bathymetric highs of rock protruding through this sediment veneer. This facies is the second least dominant geological facies, accounting for approximately 2.2 % of the exposed seafloor and is mainly inshore of outcrops of the prominent reef facies to be described below.

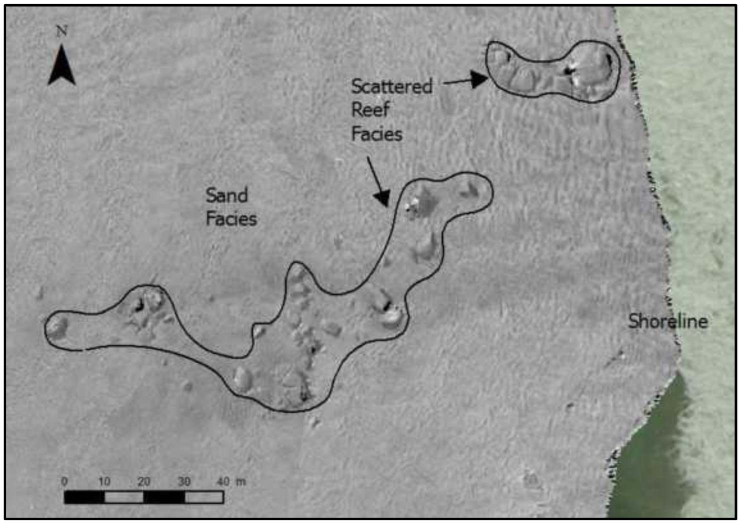

Figure 15: Surficial expression of the scattered reef facies possessing equal proportions of soft-sediment and boulder to cobble sized clasts and surrounded by unconsolidated sandy sediments

Prominent Reef Facies

The acoustic facies classified as Prominent Reef has a strong reflective pattern with well defined, large acoustic shadows indicative of a rugged microtopography (Figure 13). This facies is the dominant facies in the survey area and occupies 65.8 % of the total mapped area. The facies dominates the offshore zone, interrupted only by sediment infilled gullies. A small tombola of this facies can be found connecting the shallows on Second Beach (Priority Area 1) in the eastern and central portion of the Clifton embayment.

Sub-bottom Profiling

The reflection seismic data were collected using a DA4G. The sediment isopach surface was created by digitizing the base of unconsolidated sediment to define thicknesses of constituent packages, using in-house Council for Geoscience software, NavLog. These XYZ ASCII data were exported as text files and gridded to produce a surface of unconsolidated sediment thickness.

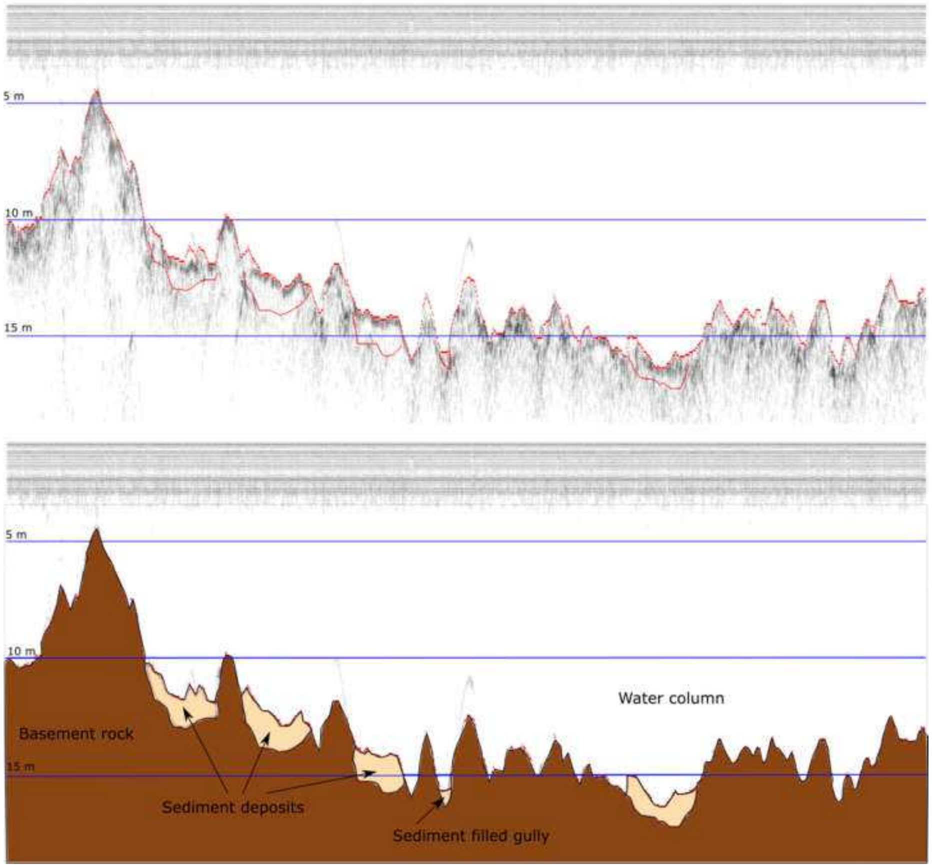

Figure 16: An example of a processed line showing a cross-section through mostly rocky basement with minor sediment pockets or gullies. The lower surface depicts where bedrock extends below sediment cover

An isopach chart displaying the thickness of sediment (isopach) cover in the area is provided in Figure 18. Sediment isopachs range from a 0 – 4.64 m. Sediment is thinnest (or absent) in the central, offshore portions of the bay and thickest inshore and towards the northern and southern boundaries of the embayment. The inshore thickening of sediment is interpreted as being a result of deposition from waves and tides as hydrodynamic energy is increasingly dissipated toward the shoreline. The thickened sediment on the northern and southern margins of the bay are a result of similar mechanism acting towards the sheltered margins of the bay where hydrodynamic energy is likewise diminished.

A relative depocentre is located on the NE corner of Area 4 (~4.64 m sediment thickness) within a deposit which extends inshore in an ESE direction. Two further maxima are located in alignment with this the same deposit in an offshore direction (both >3 m sediment thickness). Another two relative accumulations exist on the southern extent of the embayment with the deeper of the two located near the intersection between the sandy shoreline and rocky headland. Though these local depressions do exist, shallow sediment cover is the norm with approximately 50% of the surveyed mantled by a thin veneer of sediment less than 1 m in thickness.

A chart depicting the bedrock elevation is provided in Figure 19. Cross-sections running perpendicular to the general coastal trend are displayed in Figure 17, the locations of which are displayed on Figure 11. When comparing profiles from the outer margins of the embayment (Sections 1 & 4) with profiles situated more centrally in the embayment (Sections 2 & 3), it is apparent that sediment accumulates along the outer, northern and southern margins of the embayment and thins toward the center of the embayment. The basement is notably raised and irregular towards the southern extent of the embayment (Sections 3 & 4) whereas it deepens in a more gradual and uniform manner to the north. Section 4 shows the deepening of the bedrock surface away from the shoreline but then a rapid shoaling towards the sub aerial boulders forming a part of the southern headland bounding the bay.

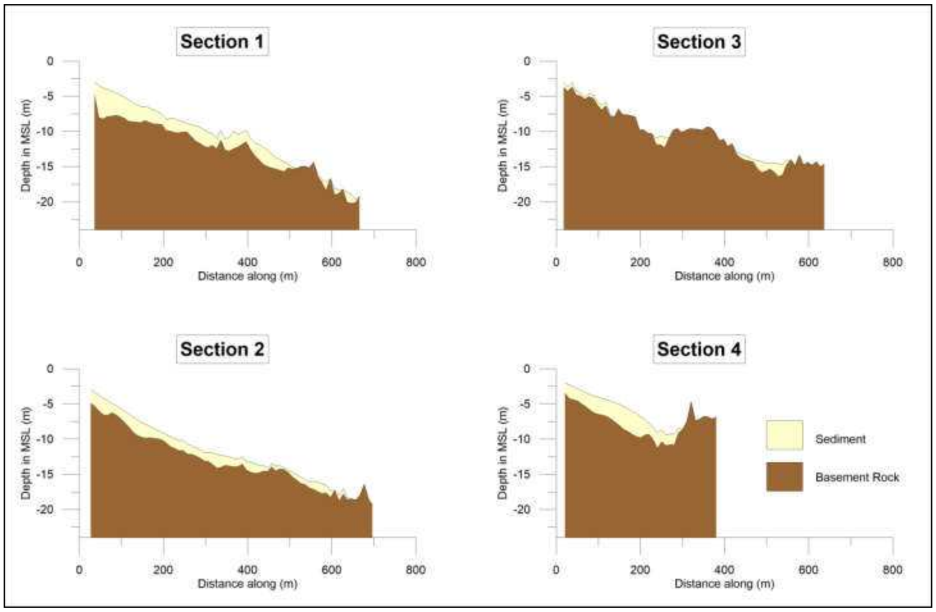

Figure 17: Cross sections 1- 4, showing sediment cover on top of Granite basement. The locations for cross-sections are displayed in Figure 18

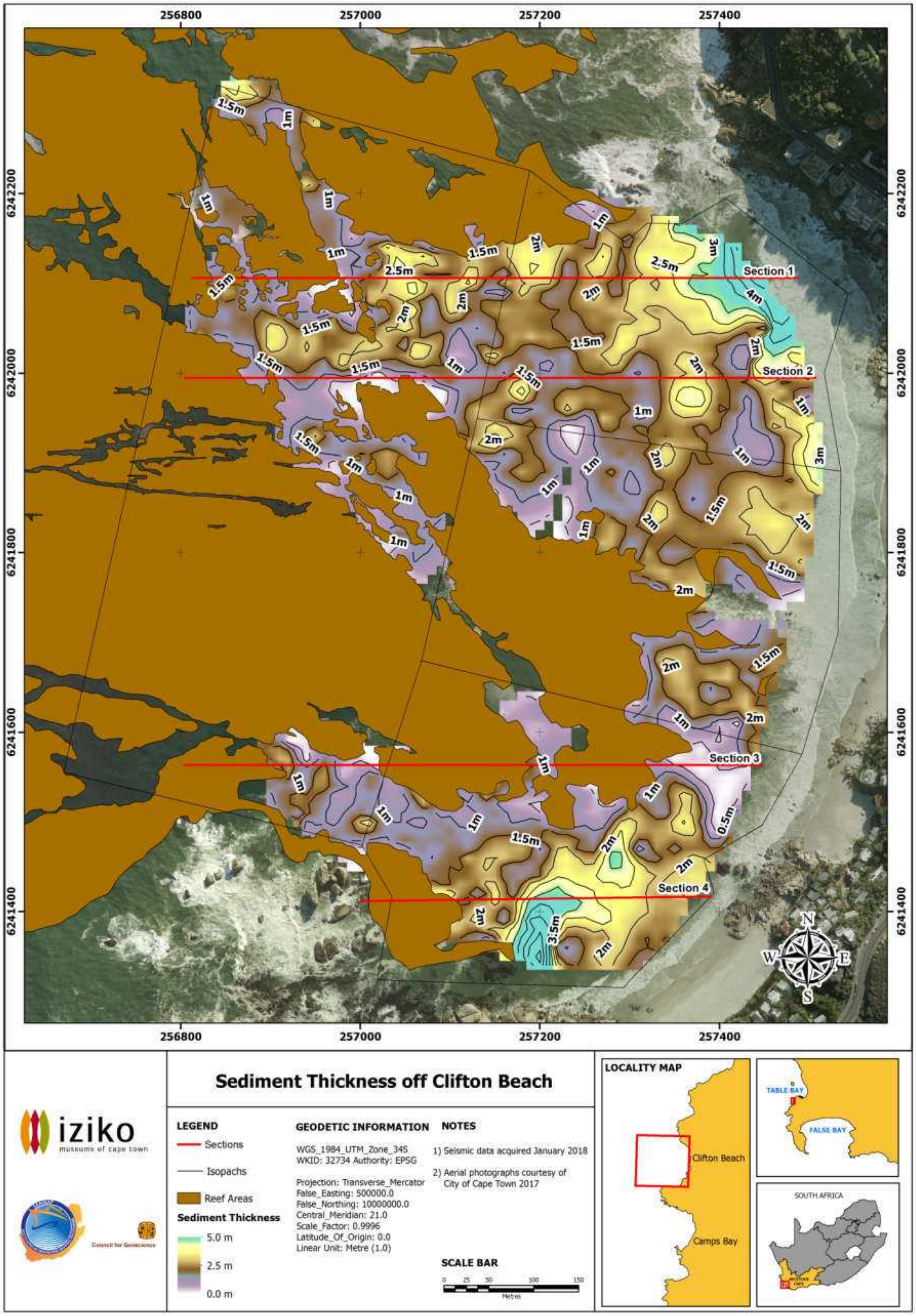

Figure 18: Isopach chart of sedimentary cover off Clifton Beach

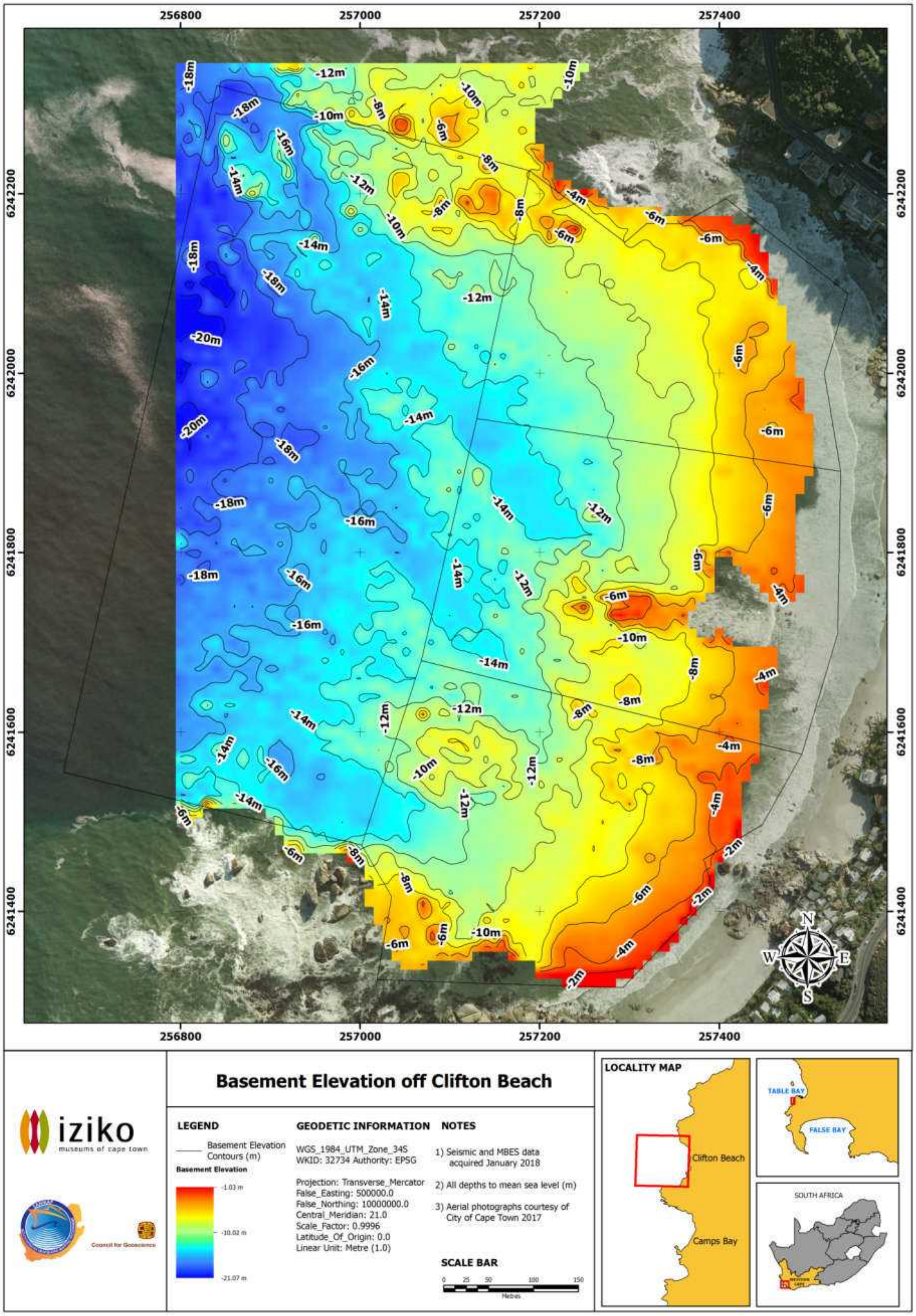

Figure 19: Chart displaying bedrock elevation within the Clifton embayment

Discussion

Basement

The basement rock exposed in the Clifton area, classified as prominent reef and scattered reef facies in the seafloor geology map, is part of the Cape Granite Suite. Granite has been mapped onshore all along the coast from Sea Point to Hout Bay (Theron et al., 1992). A typical characteristic of granite in the area is the presence of conjugate joint sets and large twinned orthoclase phenocryst within the rock. The joint sets are widely spaced, which results in the granite weathering into large boulders. Granite tends to weather by a process of exfoliation, where the surface layer peels off due to uneven heating by the sun. This results in the characteristic rounded boulders or core-stones seen along the coastline. The basement geology is responsible for the shape and morphology of Clifton. The resistant granite forms headlands on either side of the bay which results in the pocket beach of Clifton.

Sediment Transport

Sediment transport in the Atlantic Seaboard and the Clifton area is closely linked to seasonal variations in weather patterns. Sediment is generally transported by aeolian processes, wave action or currents. Wind directions control the waves with near shore currents created and controlled by the interplay between the relative directions of waves and/or wind. Wind is, therefore, ultimately the primary driving mechanism for sediment transport. In the Western Cape the seasonal weather patterns result in south-easterlies dominating in summer and north-westerlies dominating in winter season. High-energy wave conditions occur mostly during the winter from the south-west originating from winter storms in the South Atlantic. The direction of the dominant wave regime and the orientation of the Atlantic Seaboard coastline are the main factors which drive the direction of nett sediment transport. Waves predominantly hit the coastline obliquely from the south west, which result in long shore drift to the north and a corresponding northward migration of sediment. The rocky nature of the coastline, however, affects sediment transport by forming sediment traps and sediment barriers which locally impedes sediment migration along the coast.

Beaches

From previous studies in the area (Camps Bay and Sandy Bay), seasonal variations in sediment movement can be inferred for Clifton Beach. Erosion and accretion on beaches relates largely to seasonal variations in the amount of wave energy. During winter months, high-energy wave events or storms, results in erosion of beaches, while during the summer months relatively low- energy wave conditions prevail and sediment accretion occurs on the beach (Figure 20). High-energy wave events are generally associated with winter storms and it can therefore be said that sediment movement on beaches is a seasonal occurrence: during summer small waves deposit sediment onto the beach to form a beach berm and during winter large storms waves move sediment offshore to form a bar. Aubrey (1979) determined two pivotal points at -6 m and -3 m on the beach profile about which the sediment movement pivots. Repeat surveys at different seasons will determine the pivotal points for Clifton Beach (see Figure 9 for the location of these contours).

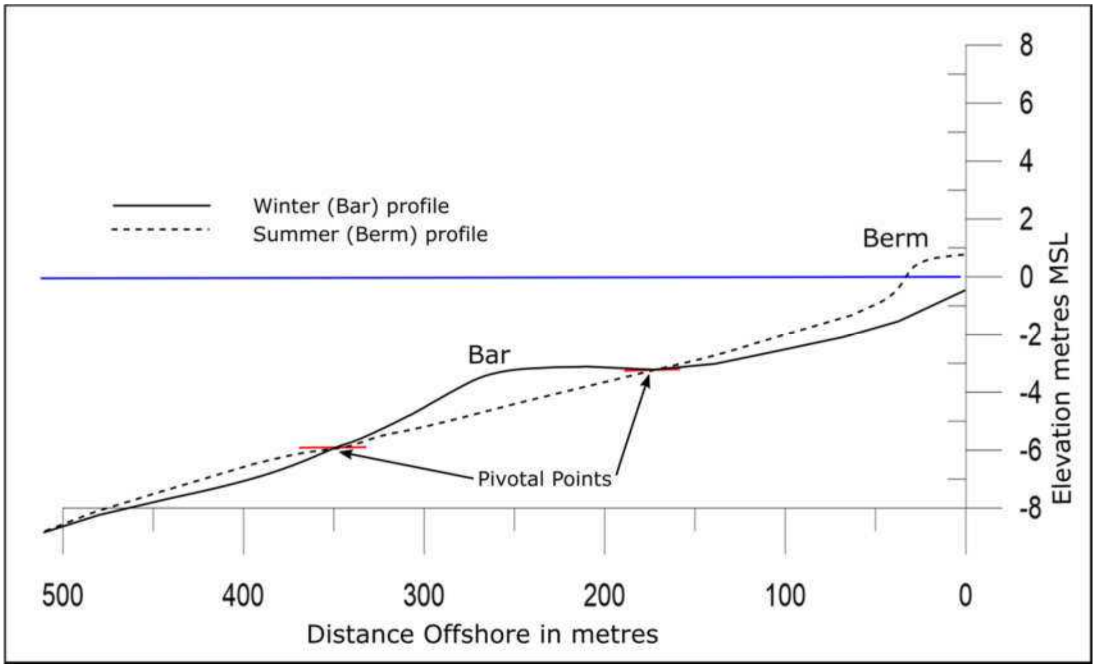

Figure 1: Winter – summer profile, during summer sediment moves onshore and forms a beach berm and during winter sediment moves offshore to form a bar, modified from Aubrey (1979)

Offshore transport

Along emergent shorelines, the presence of rocky headlands (formed by the granite basement) between adjacent pocket beaches disrupts wave-induced long shore sand transport. Headlands and reef outcrops create protected areas where the effects of storm waves are lessened and finer sediment can accumulate. Therefore, the transport of littoral sediment along a rocky coast requires a cross-shore sediment exchange and alongshore transport outside of the surf zone to bypass the intervening headlands (Tait, 1995). Storm events are generally required to move sediment offshore and past headlands for sediment to be transported alongshore (Storlazzi and Field, 2000). Sediment movement from the south by long shore drift therefore requires high energy storm events to be active and for the sediment or sand to be transported past the headlands situated to the south between Clifton and Camps Bay (Figure 21). Apart from the seasonal variation of sediment moving inshore and offshore, the sediment movement and distribution should be in equilibrium, i.e. the sediment transport occurring to the north towards Table Bay should be at the same rate as new sediment entering from the south.

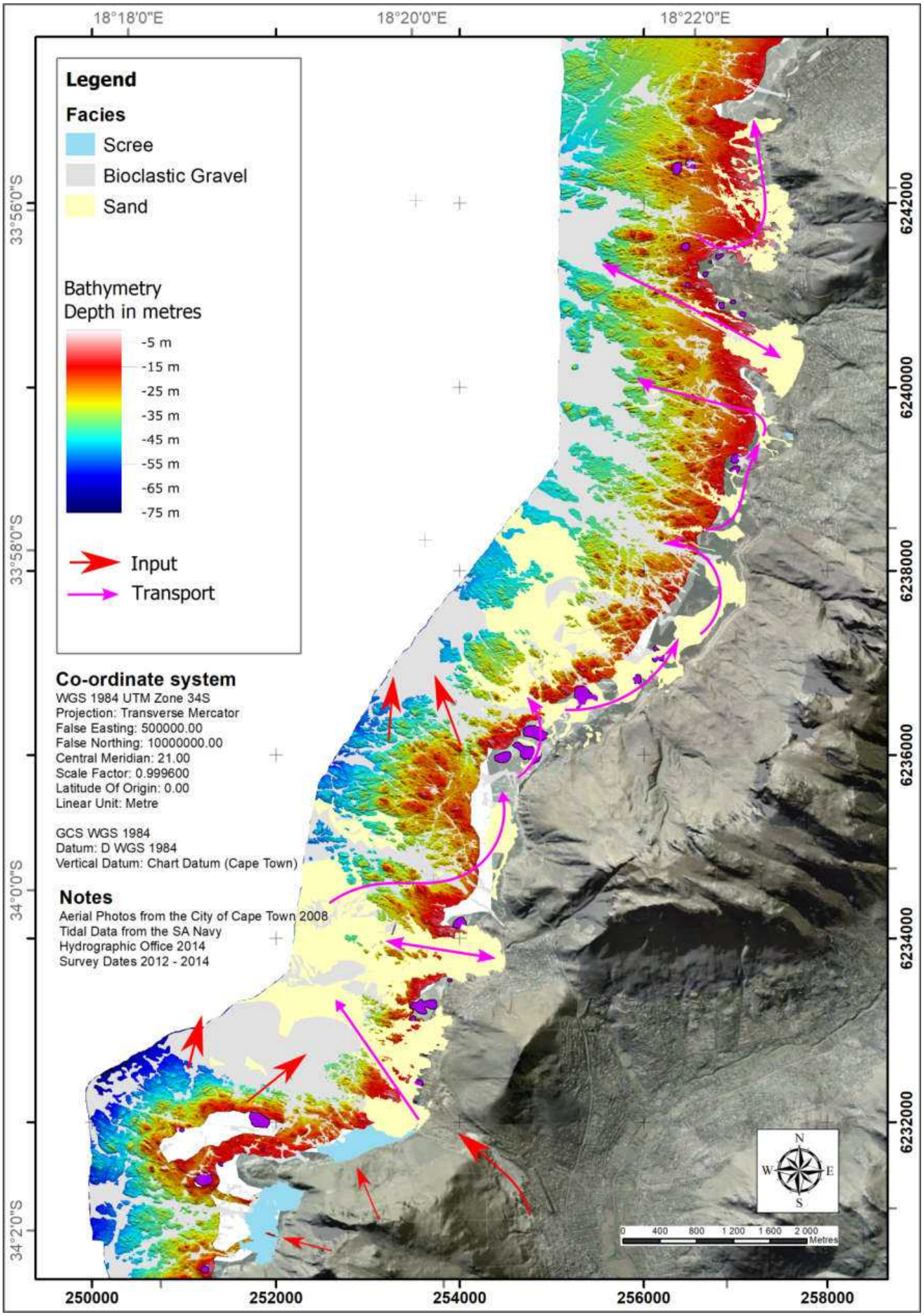

Figure 2: Sediment input (red arrows) and potential transport pathways (magenta arrows) between Sandy Bay and Clifton Beach.

Conclusion

The area is characterized by rough, high-relief bedrock comprised of the Cape Granite Suite (Rozendaal et al., 1999; Belcher and Kisters, 2003). This bedrock is highly fractured with fractures defining the orientation and width of gullies within the bedrock. The seafloor shoals towards the margins of the bay with a bowl-like geometry, deepening towards the central offshore. Sediment cover increases in thickness from the offshore to the shoreline, though exceptions occur near rocky outcrop in the center of the embayment near Second beach. In the offshore the seafloor is exposed to higher wave energy and is thus devoid of sediment cover except in the gullies. Headlands in the northern and southern confines of the embayment results in calmer inshore wave conditions which disrupt sediment transport can cause fine sediment to be deposited in these locations. These pockets have sediment accumulations of up to 4.64 m.

In order to be able to make an informed assessment of sediment dynamics of the region, a repeat study would be recommended so as to enable surfaces to be compared and centers of erosion and deposition to be identified. It is recommended that follow-up surveys be performed at quarterly intervals so as to better assess seasonal fluctuations and sediment migration patterns within the Clifton embayment and surrounding the vessel remains. This will allow the sediment dynamics at Clifton Beach to be better constrained.

References

Aubrey, D. G. (1979). Seasonal patterns of onshore/offshore sediment movement. *Journal of Geophysical Research* **84** (C10), 6347-6354.

Belcher, R.W. and Kisters, A.F.M. (2003). Lithostratigraphic correlations in the western branch of the Pan-African Saldania belt, South Africa: the Malmesbury Group revisited. *South African Journal of Geology*, **106,** 327-342.

Rozendaal, A., Gresse, P.G., Scheepers, R. and Le Roux, J.P. (1999). Neoproterozoic to early Cambrian Crustal Evolution of the Pan-African Saldania Belt, South Africa. *Precambrian Research*, **97**, 303-323.

Schimel, A.C.G., Beaudoin, J., Gaillot, A., Keith, G., Le Bas, T., Parnum, I. and Schmidt, V. (2015). Processing backscatter data: From datagrams to angular responses and mosaics. *In:* Backscatter measurements by seafloor-mapping sonars – Guidelines and Recommendations, 133-164.

Storlazzi, C.D. and Field, M.E. (2000). Sediment distribution and transport along a rocky, embayed coast: Monterey Peninsula and Carmel Bay, California. *Marine Geology* **170** (3-4), 289-316

Theron, J.N., Gresse, P.G., Siegfried, H.P and Rogers, J. (1992). *The geology of the Cape Town area*. Explanation on Sheet 3318, Geological Survey, South Africa. 140 pp.

Tait, J.F. (1995). *Rocky coasts and incerse methods: sediment transport and sedimentation patterns of Monterey Bay National Marine Sanctuary*. PhD thesis, University of California at Santa Cruz, California, 138 pp.

Follow up Survey, October 2018

Multibeam Bathymetry

The multibeam data for the follow up survey were collected using the same geodetic and projection parameters as the original survey, which was in WGS 84 spheroid and UTM 34 South projection. The January survey were levelled against the SAGEOID2010 (relative to mean sea level, MSL) during post processing. The June survey were levelled to the same vertical datum by lowering the surface to matchup prominent reef outcrop features. An adjustment of 0.5m were required, to adjust from the tide based port datum (Cape Town) to SAGEOID2010 land levelling datum.

Data were acquired to as close as possible to the shore line, keeping the vessel and equipment safe. Due to a lower tide and larger waves, the coverage did not extend as close inshore during the June survey as during the January survey. As the survey progressed and the tide receded small gaps remained which could not be covered due to safety reasons. With the interest being mostly on the inshore the survey did not extend as far offshore, as it was determined to consist mostly of exposed reef during the January survey.

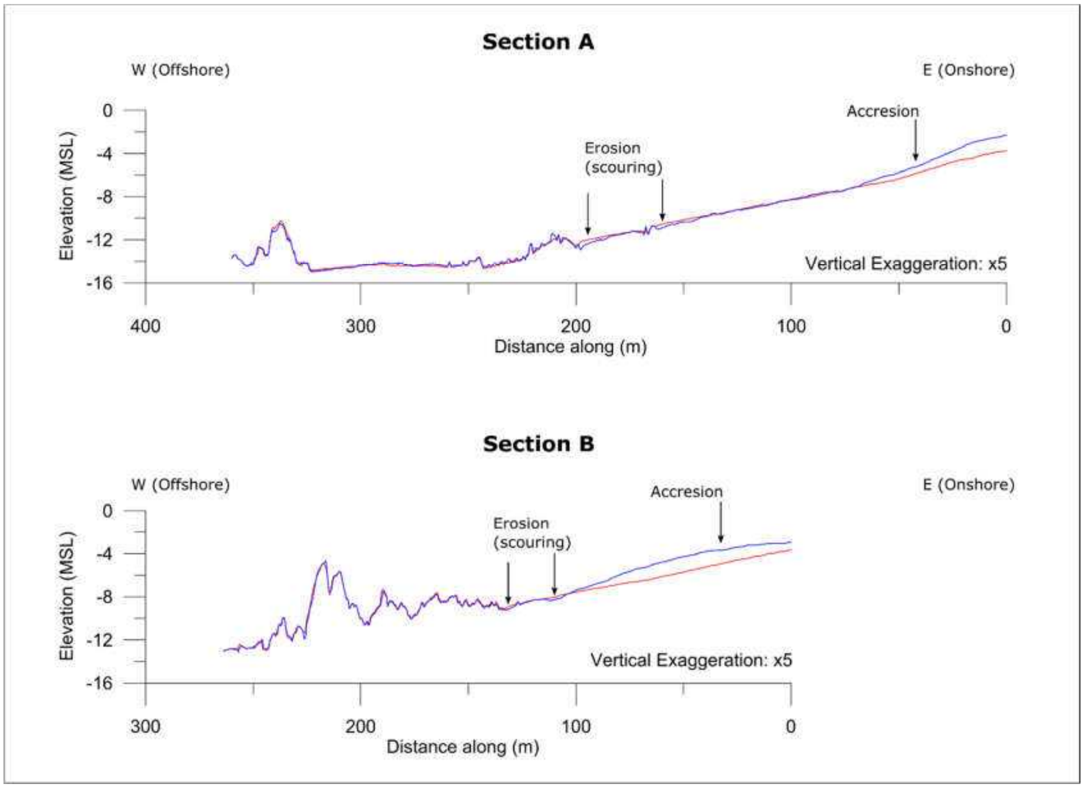

Figure 4: Graph showing the change in elevation of the seabed between January (red line) and June (blue line) along Section A and Section B

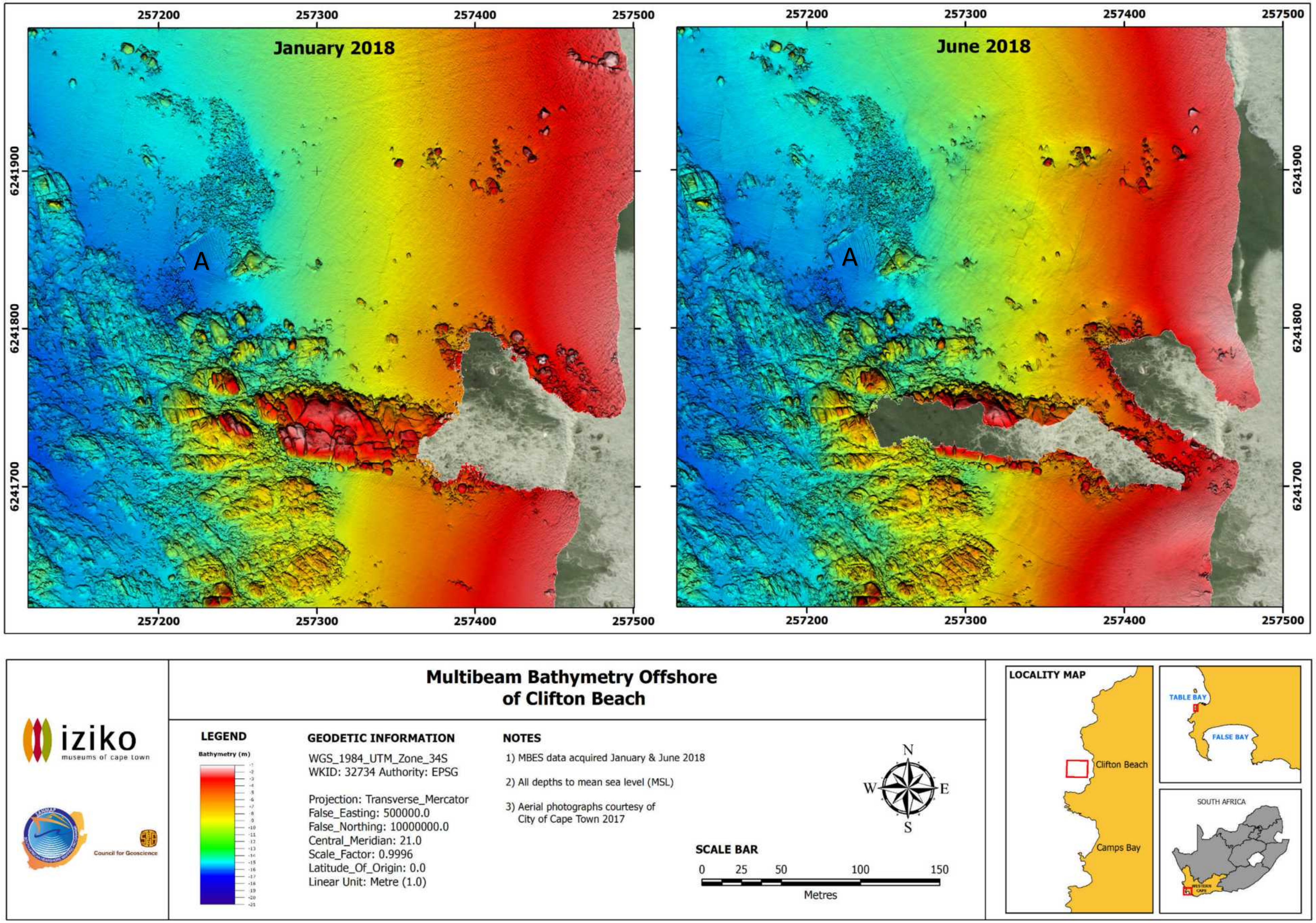

Figure 5: Comparison of January and June multibeam bathymetry results in the area of interest.

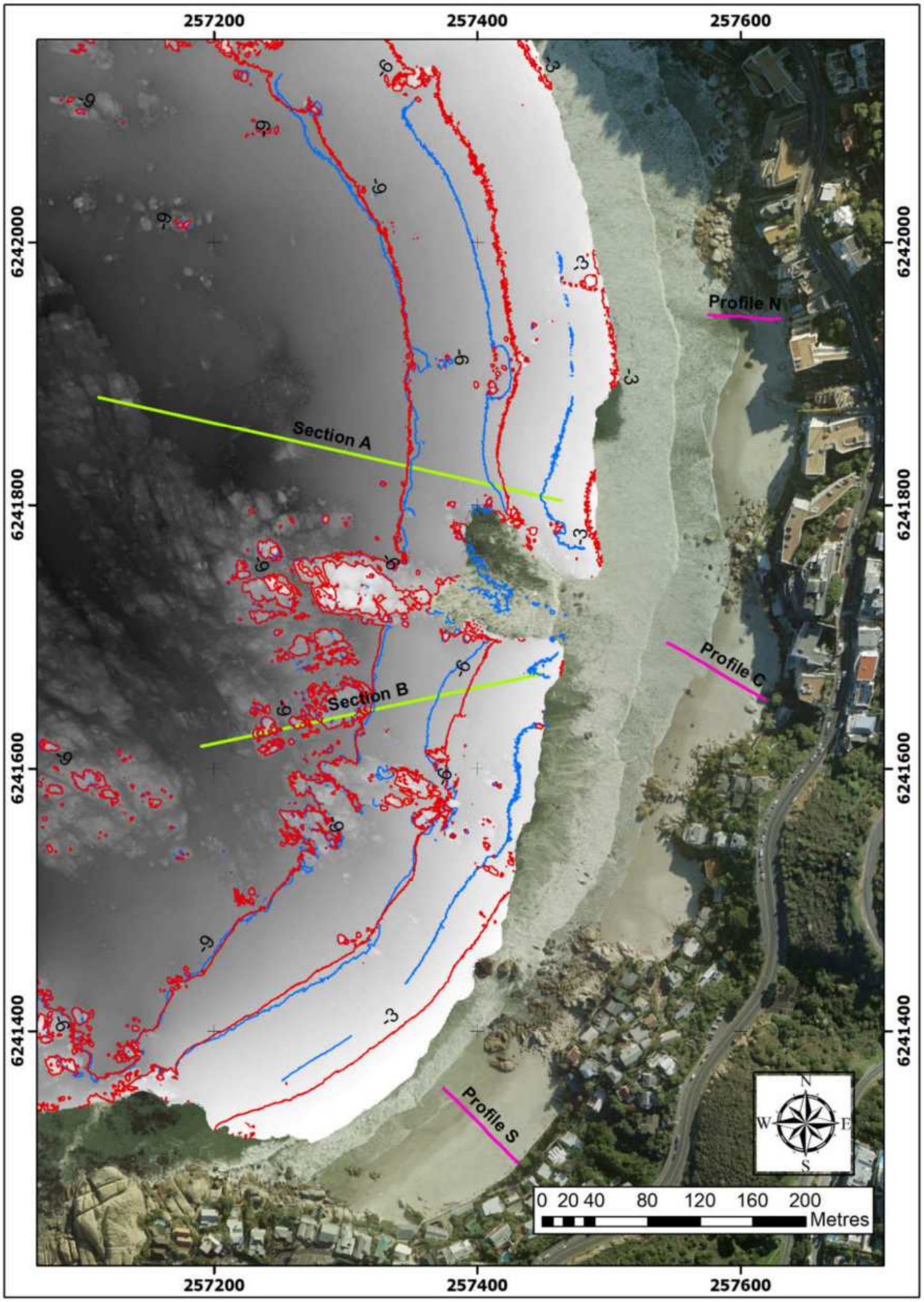

Figure 6: Comparison of January contours (red) and June contours (blue)

Comparing the January and the June surveys, the following general trends can be observed; an increase in sedimentation was observed on the inshore of the survey from January to June. This can be observed mostly between the -3m and the -6m contours. Further offshore from -8m and deeper minor scouring can be observed. This is mostly evident around reef outcrops and the boulder beach identified in the January report. This can be confirmed by comparing the -3, -6 and -9m contours. The -3m and the -6m contour migrated offshore during June, indicating a shallowing of the seafloor. This horizontal shift of the contour was up to 35m in places. The -9m contour shifted only a few meters, both offshore and inshore, and some places remained static.

Volume calculations between the January and June surveys were conducted using Surfer. Cut (sediment accretion), fill (Sediment erosion) and nett volumes changes were calculated with the following results:

Cut (Accretion)	54 626 m^3
Fill (Erosion)	20 105 m^3
Net volume change	34 521 m^3

Calculations are based on overlapping grids where there are data for both surfaces only and ignores blanked and no-data area in either surface.

Shore face slope

The shore face slope for January and June were calculated using the sections shown in Figure 4. During the June survey there was a marked increase in the slope of the shore face. The average slope from the January survey was measured at 4.0 % and increased to an average of 6.4 % during June.

Bioclastic gravel with ripples

An area of bioclastic gravel with wave ripples have been identified to the north of the central reef extending offshore from 2nd beach. The area consists of a ripple field roughly 32 m long by 20 m wide. A profile across the January survey shows wave ripples (symmetrical) with an average wave length of 1.4 m and an amplitude of 0.15 m. During the June survey the average wave length and the amplitude increased to 2.7 m and 0.25 m respectively.

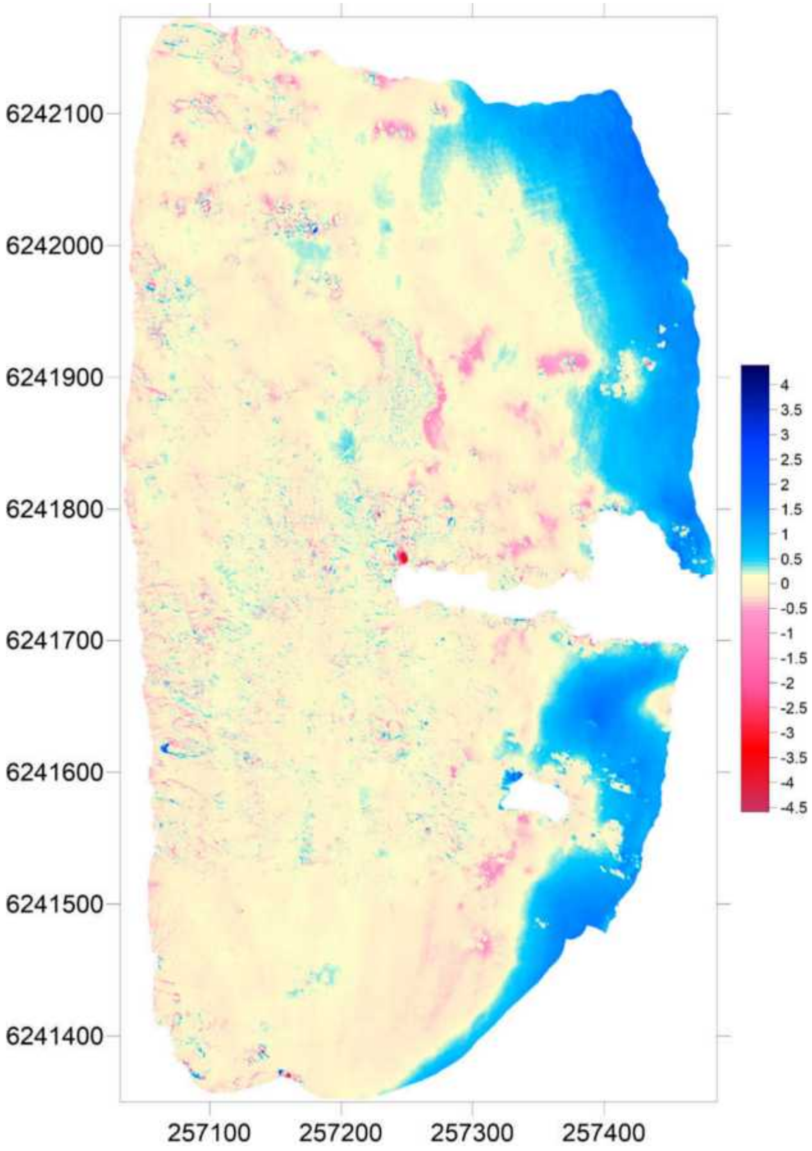

Figure 7: Positive changes (accretion) in volume shown in blue and negative changes (erosion) in red, while no change is in yellow

Beach profiling

Mothly beach profiling were conducted by IZIKO staff, using post prosessed RTK positioning. Three profiles are conducted in the same location each month. The profiles are Labled N, C and S located on First, Second and Fourth beach respectivly (Figure 6). All three profiles indicate errosion of the beach between January and June. The level of errosion varied between the different profiles and ranged between 0.5 m to 1.5 m. Even though the beach level decreased from January to Jun, the average sloped remained very similar at 7 % ±0.5 %

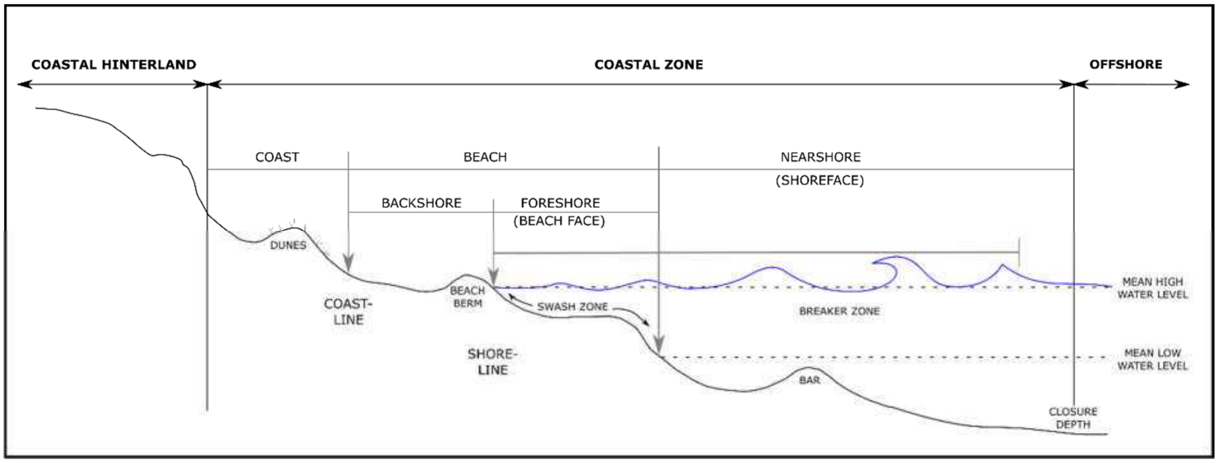

Figure 3: Diagram of a beach profile with processes shown, modified from (Komar, 1998; USACE - CERC, 1984)

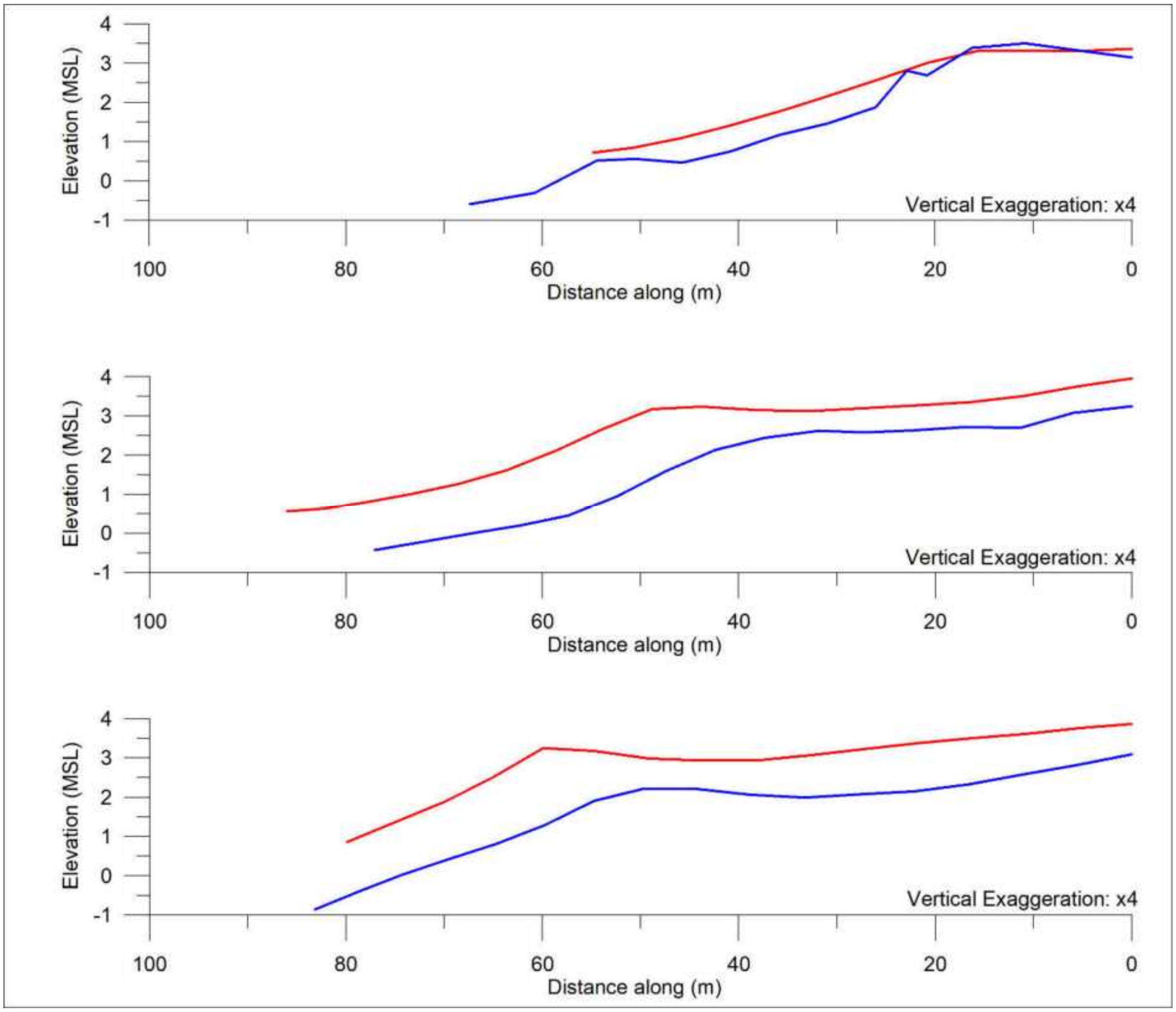

Figure 9: Beach profiling conducted by Iziko. January lines in red and June lines in blue

Discussion & Conclusion

When analyzing the offshore and the beach data between January and June, erosion took place between 3.5 m and -0.5 m elevation on the beach and accretion took place in the shallow water between -3 m and -6 m. It is there for concluded that sediment which were eroded from the beach during winter, is deposited close inshore on the shore face to form submerge sand bars or sand banks (**Figure 8**). The reverse is expected to happen from winter to summer where sediment from the shore face would be transported onto the beach. The movement of sediment from the beach to the shore face is mostly a function of the wave energy during storm events. During large storms the high energy wave condition s remove the sediment from the beach and deposit it further offshore. The opposite happens during calm low energy conditions, where sediment is transported onto the beach from the shore face. Because most large storm events occur during winter this movement of sediment between the shore face and beach cycles though a seasonal basis, where erosion of the beach occurs mostly during winter and deposition of sediment occurs during summer (Van Zyl, 2018).

Evidence for increased wave energy during June can be seen in the wave ripple field shown in Figure 5 labelled “A”. An increase in wave length and amplitude of wave ripples in the same water depth is an indication of an increase I wave height (Evans, 1942).

References

Evans, O.F., 1942. The Relation Between the Size of Wave-Formed Ripple Marks, Depth of Water, and the Size of the Generating Waves. SEPM Journal of Sedimentary Research Vol. 12. https://doi.org/10.1306/D4269139-2B26-11D7-8648000102C1865D

Komar, P.D., 1998. Beach processes and sedimentation, 2nd ed. ed. Prentice Hall, Upper Saddle River, N.J.

USACE - CERC, 1984. Shore Protection Manual. Department of the Army, U.S. Corps of Engineers, Coastal Engineering Research Centre, Washington, DC 20314.

Van Zyl, F.W., 2018. Geological mapping of the inner shelf off Cape Town’s Atlantic Seaboard, South Africa (MSc). University of Cape Town, Cape Town.

Van Zyl, F.W., Salzmann, L., Pillay, T., 2018. Geophysical Investigation Off Clifton Beach, Cape Town (GTP No. 2018– 0004). Council for Geoscience, Bellville.

Beach dynamics

This section includes the information collected in the field by Iziko staff and interpretation by the environmental consultant Dr C. Wainmann.

EROSION AND ACCRETION USING ARCHIVED GOOGLE EARTH IMAGES

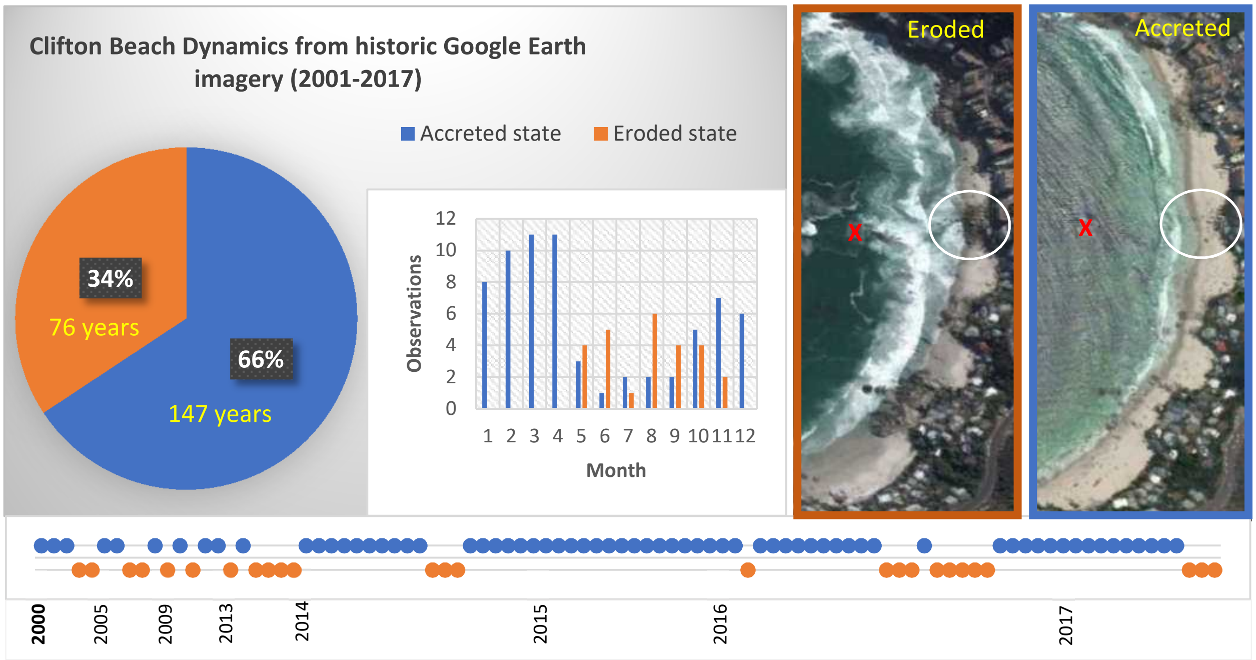

Google Earth provides historic satellite derived visual images of the earth surface. In this instance these images were used to characterize past accreted/eroded states of the beaches in Clifton Bay. Eroded conditions are those where the rocks at the 4 headlands are exposed during winter months. In contrast, accreted conditions are evident for the same rocks that become buried by beach sand during mostly summer months. An example of this is shown by the white circle shapes in the image above. The red “X” denotes the wreck site.

The above Google Earth images show the exposed and sand covered rocks at 2nd Beach Clifton, on the shoreward side of the wreck site, in a state of Erosion and Accretion respectively.

94 Images, between 2001 and 2017 were extracted from Google Earth's Historic records of Clifton Bay and examined for their eroded/accreted status. Where records of the same status existed, the number of days for each contiguous status type was then accumulated. 534 Days or 34 %, of the total days displayed eroded conditions. In contrast, 1023 days or 66 %, of the total days displayed accreted conditions at the site. When extrapolated, the persistent mechanical winter swell has impacted the wreck site for 76 years of the 223 years since the wrecking of the *São José*.

From the histogram plot it is evident that erosion occurs predominantly between months of May and November, whilst accretion occurs ubiquitously but predominantly between October and April.

Of the 36876 days that occurred from the first image on 16 December 2001 to 26 August 2017, 94 images were available for interpretation, representing only 0.25 % of time-window coverage. The temporal coverage of the dataset is also biased to the last 4 years, when these images were collected more frequently. Another factor that influences such image opportunities is the cloud cover criteria, since this visual band cannot penetrate cloud.

One is reminded that this is a scarce data set and interpretation should be treated with caution. However, this is the only tempo-spatial record that exists for the site and was hence considered important to be included here, especially as a hind casting proxy tool.

Beach Profiling

Cross-shore beach transects of elevation are a useful method for characterizing and quantifying sand erosion and accretion, as is known to occur at the wreck site. 3 Transect lines, at the 'Northern' (1st Beach), 'Central' (2nd beach) and 'Southern' beach (4th beach) were undertaken. These are shown on the map in the figure below.

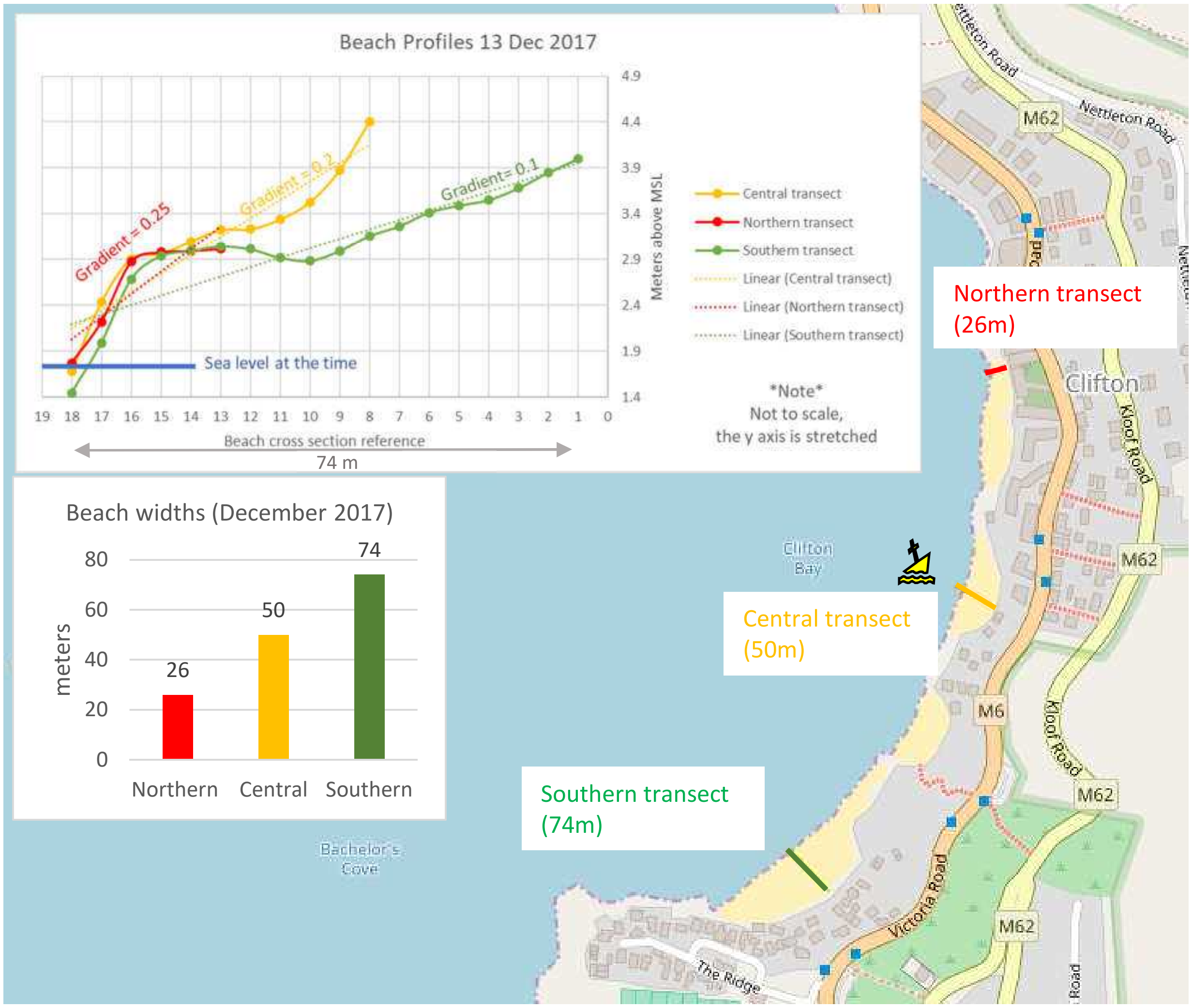

From the beach profiles undertaken on the 13 December 2017, it is evident that the shortest Northern transect line represented the narrowest of the 3 beaches measured. A cross section beach length of 26 m was measured. This most narrow beach is due to the perpendicular orientation of the coast to the prevailing south-westerly swell direction. This small segment of the coast is also completely exposed to the incoming swell, since there is no protection offered by the southern headland at Maidens Cove. Swells that impact the beach are generated 1000s of kilometers away in the deep oceans by strong, persistent winds, blowing across an extensive water surface.

A gradient of 0.25 was measured for the Northern transect line and was the steepest of the 3 transects undertaken.

The Central transect line bisects Clifton 2nd Beach, also perpendicular to the shoreline. Its gradient was determined to be 0.2. This was somewhat reduced due to the increased ‘bending’ or refraction of the prevailing south-westerly swells as they travel around the Maidens Cove headland. This extra travel distance and steering of the waves reduces the energy component somewhat that results in lesser erosion of by swell events, which turn results in a slight increase or accretion of beach sand. This increased accretion determines the width of the beach that was measured as 50 m from the water’s edge to the eastern extremity of the beach on 13 December 2017.

The Southern transect also bisects its beach, commonly known as Clifton 4th Beach. This represents the south-western extent of the greater Clifton Bay and is significantly protected from the prevailing south westerly swells by the extended headland to the west. This is the most popular tourist beach. A wide cross section beach length of 74 m was measured. Waves that impact this beach are significantly smaller than those at 1st Beach about 800 m northwards, that has contributed the permanent greater width of this beach. Its gradient was determined to be 0.1.

A cross-sectional beach transect of 50 m in length was undertaken a month apart during November and December 2017, using 13 and 11 points along the line respectively. These are shown in the figure below as Purple (November) and Orange (December) lines, with their measurement reference numbers. Point altitudes along these lines were measured using a Trimble Real Time Kinematic (RTK) GPS, owned by Iziko Museums.

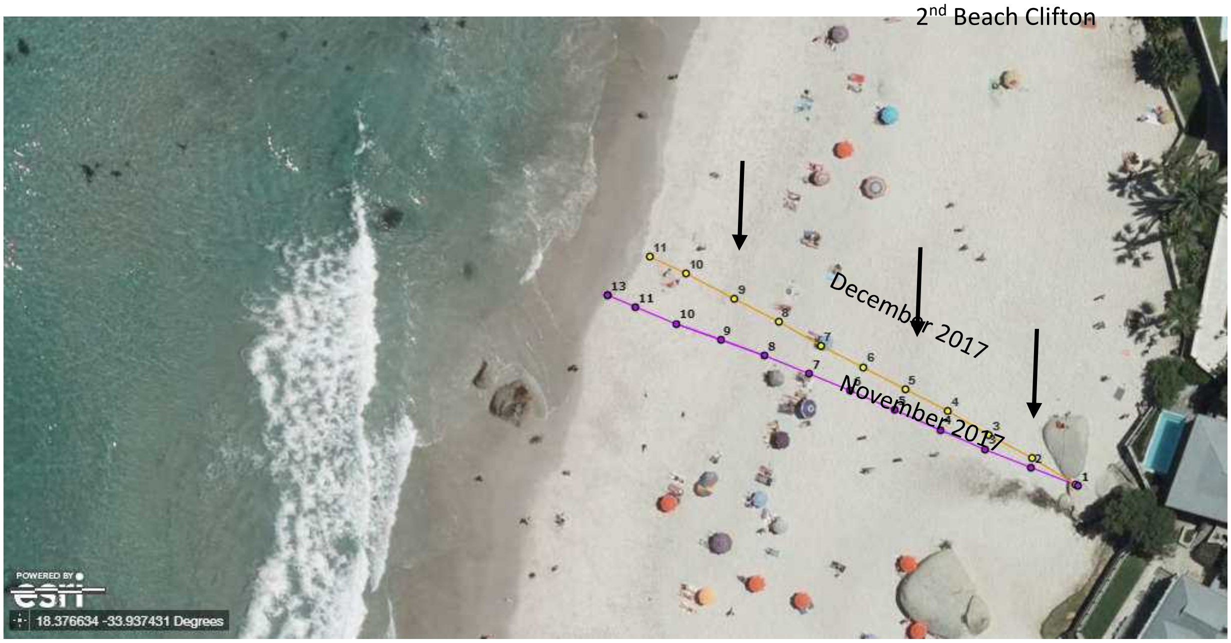

When comparing the corrected altitudes for these Central Beach transect lines, between November and December 2017, an accreted depth of 0.02 m to 0.4 m was noticed between measurements numbers 7 and 8 and numbers 10 to 11.

Similarly, an accreted depth of approximately 0.6 m occurred between measurement numbers 9 and 10. Using the wet sand demarcation line from the high-resolution aerial image we were able to deduce the approximate water line, although the image was taken early in 2017. These results can be seen in the plot below.

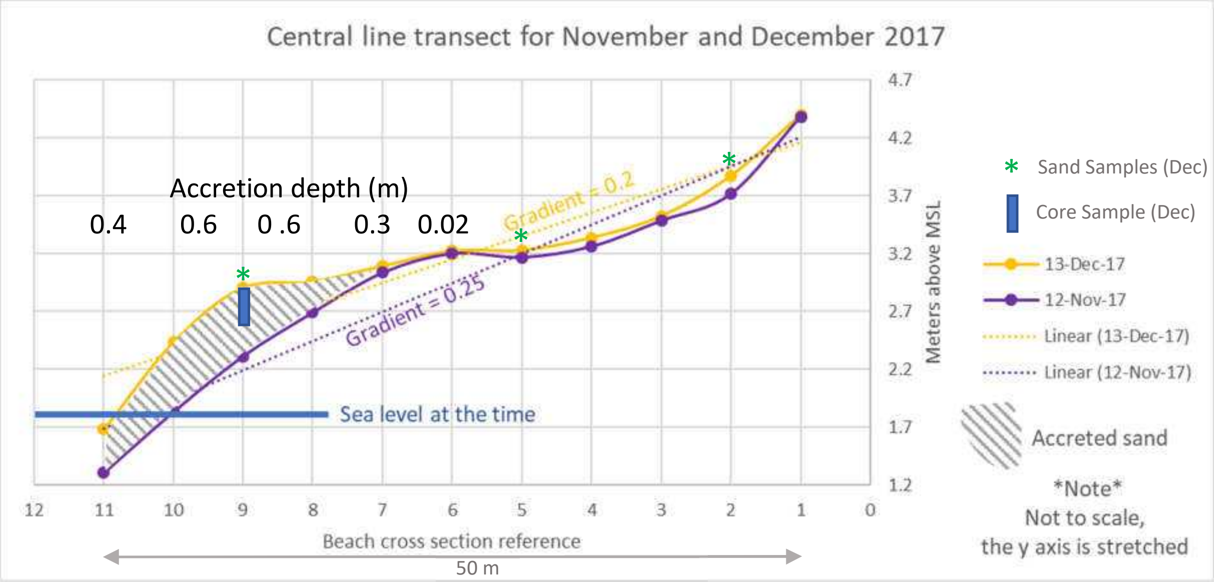

Using the single transect line as a guide and applying the same ratios of accretion for that line, it was possible to interpolate the accretion depths for the remainder of the Central beach (2nd beach). This result is shown as orange and yellow shaded regions in the figure below.

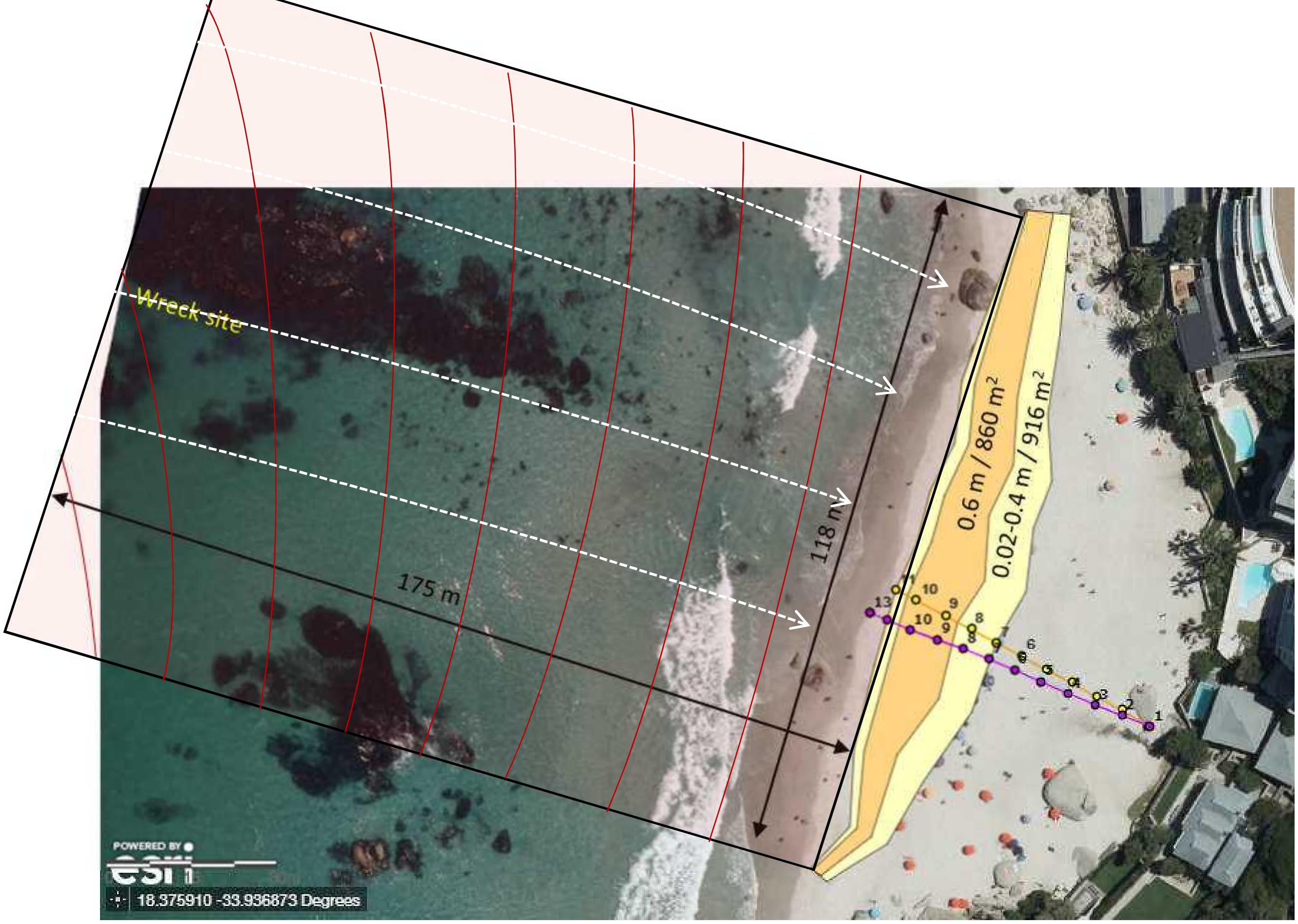

Approximately 860 m² and 916m² surface area was measured using a GIS map and is shown as polygons in orange/yellow shades. When considering the length of the beach (118 m), the distance from the accretion to the wreck site (175 m) and the surface area and depth of the accretion, it is possible to estimate the volume of overburden that took place over the 30-day period between these transect measurements.

This accreted sand overburden equates to approximately to 516 m³ and 274 m³ surface area for each polygon in the figure above and a total of 791 m³ for the entire Clifton 2nd Beach. It is likely that persistent low-energy wave action (as well as some long shore drift) resulted in the suspension and shoreward transport of finer sand grains, finally resulting in the accretion of this sand in the shaded polygon areas as shown in the figure above. If this accreted sand originated from the wreck site 175 m seawards and 118 m wide, then it would account for an average bed load depth change (erosion scour) of 30-40 mm over the wreck site area. This estimated erosion area is shown as a shaded red area in the figure above. Although this should be confirmed by further measurements, it is an important outcome since it has a direct impact on the changing absolute depth of the wreck artifacts.

The gradient change that occurred over the 30-day period from 12 November to 13 December 2017 was determined as 0.05, equating to a gradient reduction of 0.0167 per day with an average rate of accretion at 23 m³ of beach sand per day.

A simplified schematic of wave refraction for the prevailing wave field direction over the wreck site is shown as red curves in the figure above. These are the low energy summer season waves that perpetually transport the seafloor bed load shore-wards in the direction as shown by the broken white line curves. The depth at which these waves interact with the seafloor, their ability to uplift the bed load and related sand grain sizes are dealt with in the next section.

In the 2 late summer months that followed (Jan, Feb 2018), the survey distance offshore increased for the Central transect line, due mainly to being selective about the tidal height. These Beach Surveys are shown in the figure below.

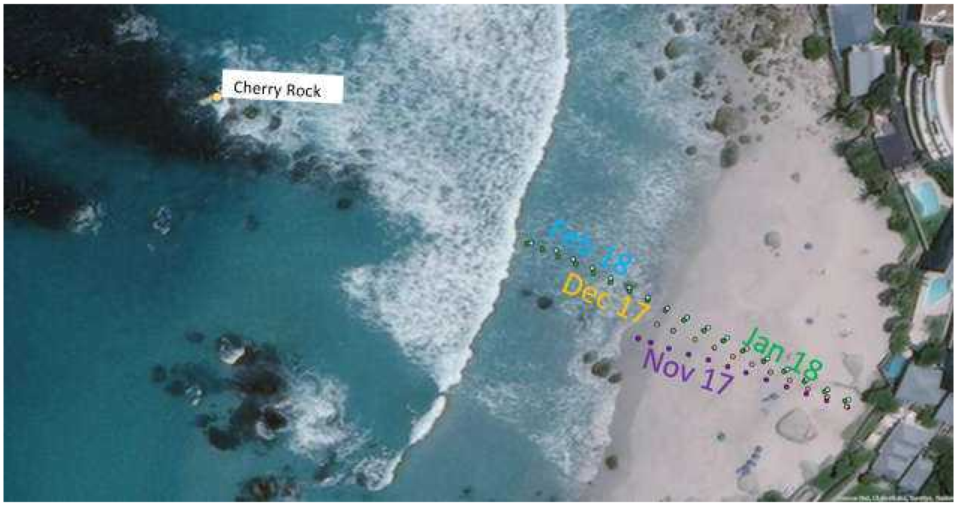

Since only the first 11 shoreward data points of the Central transect line were those that overlapped spatially for Nov 17 to Feb 18, it was convenient to plot them on the same x-axis as shown in the figure below. The incremental accretion of the beach is clearly evident as seen in the reducing gradient lines from 0.25 in November 2017 to 0.045 in February 2018. The accretion changes were all noticed in the inter-tidal zone.

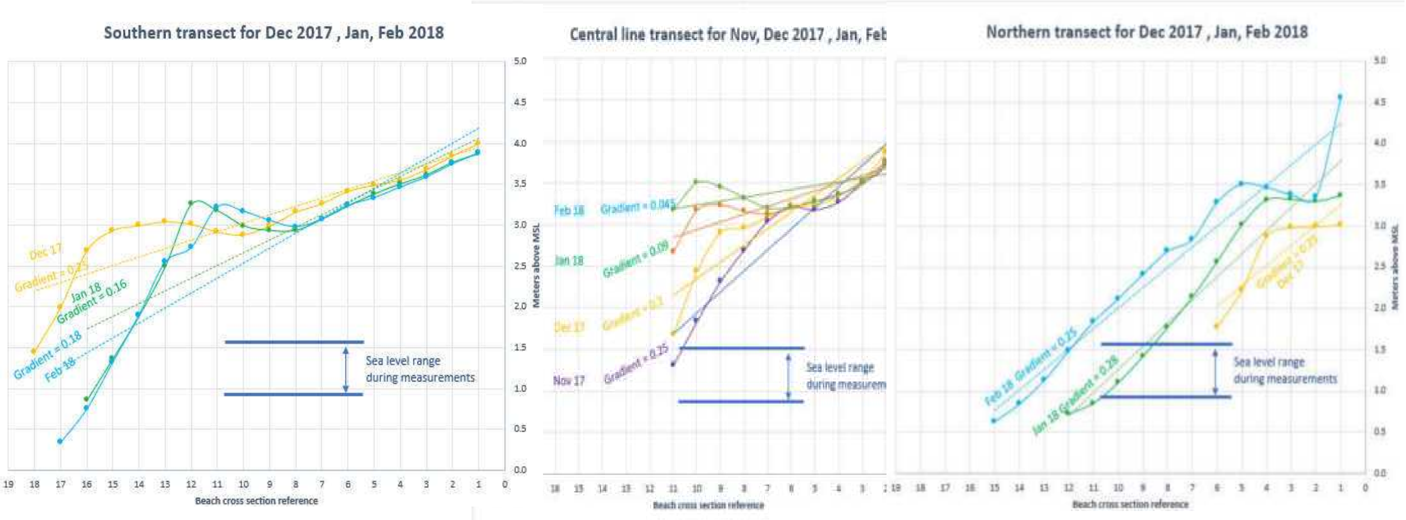

The persistent accretion of beach sand during the first 4 months of monitoring can be seen in the figure below as a hashed and speckled region of the plot. It is interesting to note the offshore extend of this inter-tidal sediment transport dynamic probably took place at reference point #17, indicating a 'null' where no significant height change occurred for that time span. It should be noted that the plot is not to scale, as the x-axis is significantly reduced to show the accretion as a schematic.

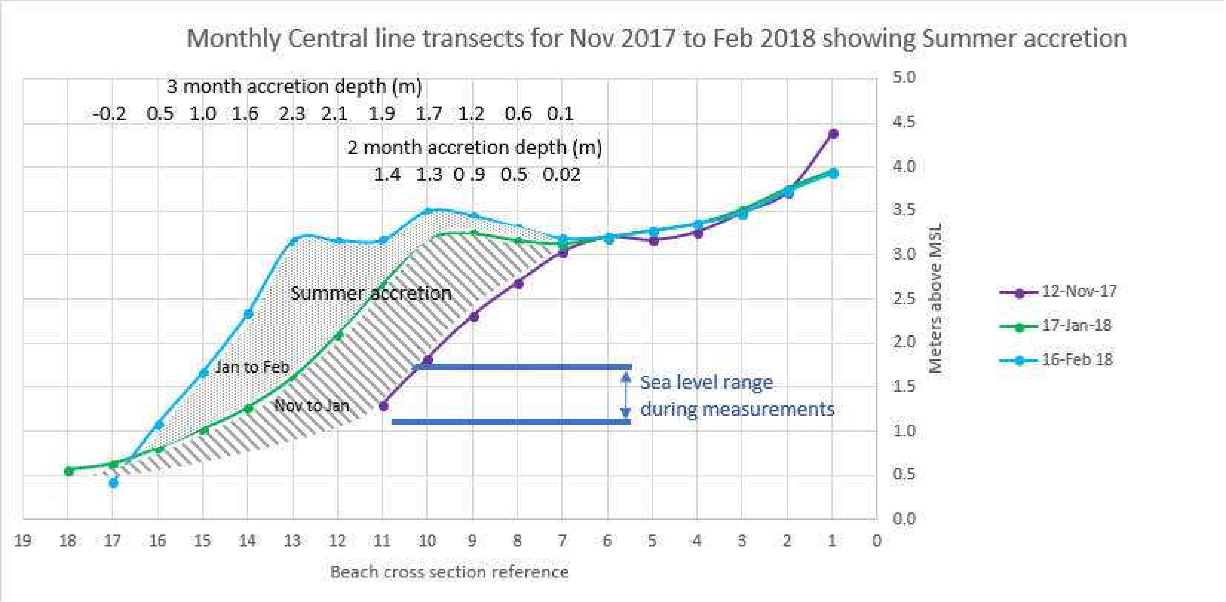

All beach transect lengths were captured into a Geographic Information System (GIS), allowing for accurate spatial representation and analysis. From the plotted transects, each line length was measured according to the start and end extremity of each line. During the surveying, each start location of each transect line was kept to the same locality. The lengths of the transects were seen to vary in accordance with the cross-sectional plots seen in the figure above. The rate of accretion can therefore be seen in the increasing cross-sectional length of each beach. This result is synonymous with the Google Earth imagery study (2001-2017) as shown earlier that showed accretion to occur during the same months.

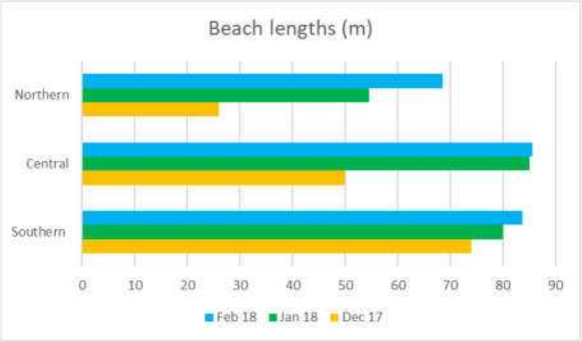

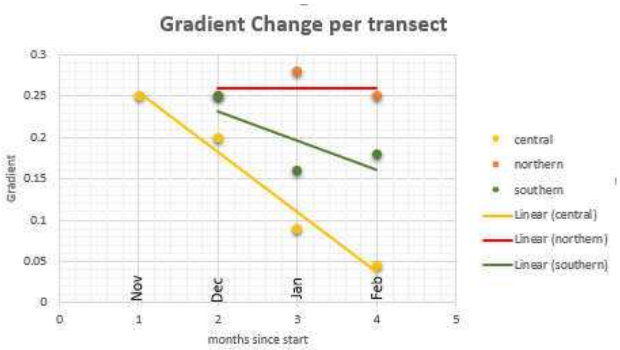

The central sector of Clifton Bay experienced the greatest gradient decline over the past 4 months since the start of the monitoring. Accretion dominated in the central and southern region of Clifton Bay whilst it showed negligible change in the northern sector. The northern line was noticed as the most stable of the 3 beaches in the study. It is likely that that the maximal accretion of sand noticed in the central transect was due in part to the protection offered by the nearby offshore reef. The same reef that caused the final wrecking of the *São José*.

Although persistent summer accretion of beach sand during the first 4 months of monitoring was noticed, the autumn months were clearly transitional as both erosion and accretion are seen in the plot below. The accretion can be attributed to periods of the low wave conditions typically known to occur during this season. However, autumn is also the time when early winter storm accompanied by large high-energy waves start battering this coast. It appears that these high-energy wave events were responsible for the erosion as seen in the dark grey speckles shaded area between February and April 2018

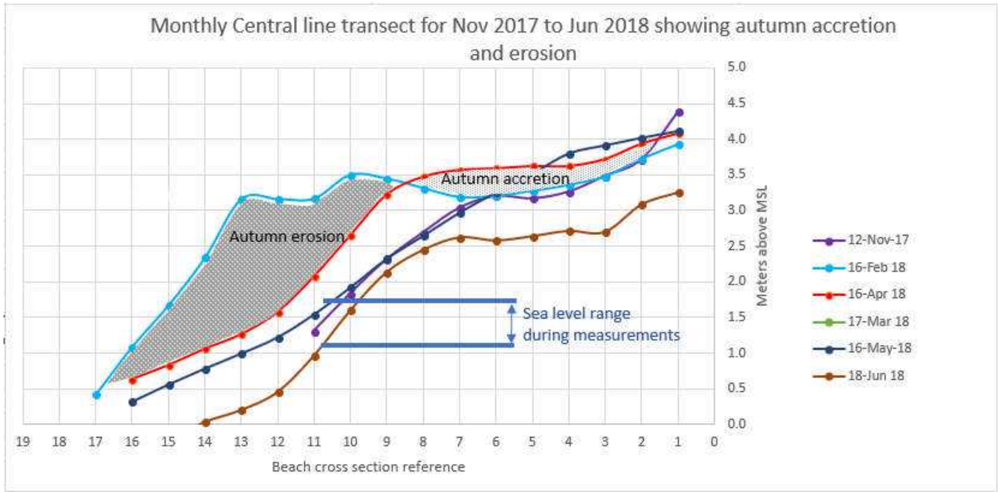

The winter season in the Western Cape of South Africa is synonymous with Cape Storms, hence the region of the shipwreck is known as the “Cape of Storms”. The pictures below were screen grabbed from a social media (Facebook) posting of Clifton Bay on the 7 June 2018 by [Michael Smorenburg](). This shows the coastline being battered by a typical winter storm. The erosion of the beach sand that accumulated in summer months can be seen by the sandy color of the waves in these pictures.

It is these storm events seen in the pictures above that occurred about a week prior to the June 2018 beach profile measurement shown in the plot below and is likely the main contributor to the winter erosion at this stage that has completely removed all the former accreted sand.

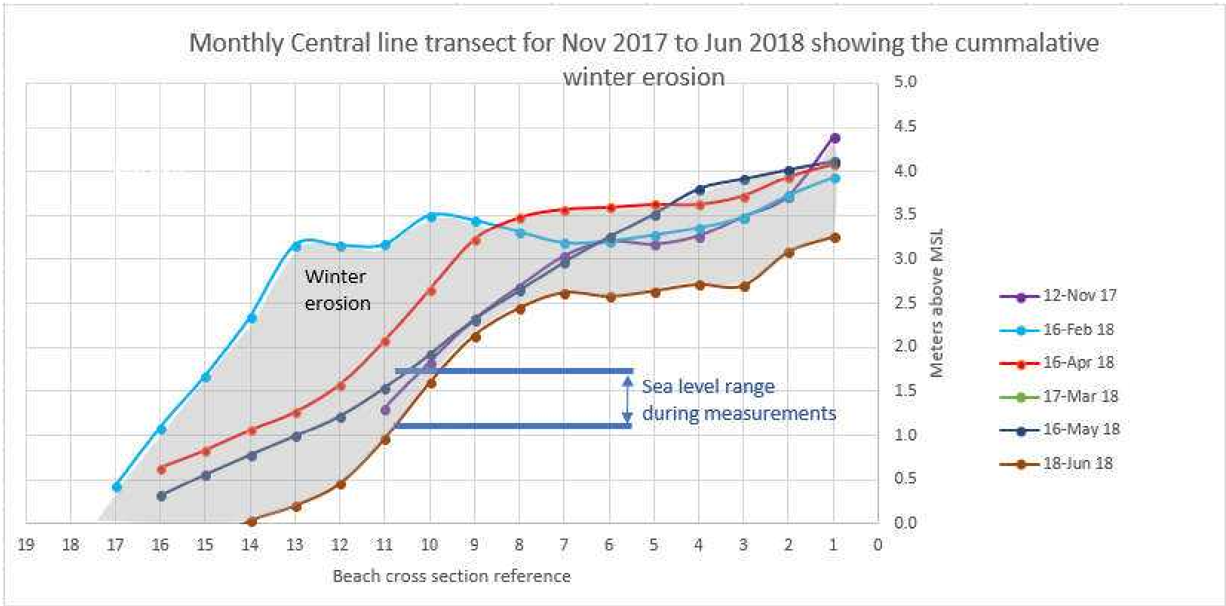

Analysis of the Northern and Southern profile lines, as shown here for the Central profile line had not been undertaken at the time of updating this report since the far field wave data is awaited that should be combined with the interpretation of these results. This will be undertaken towards the end of the 4 season’s measurement period.

Sand Sampling

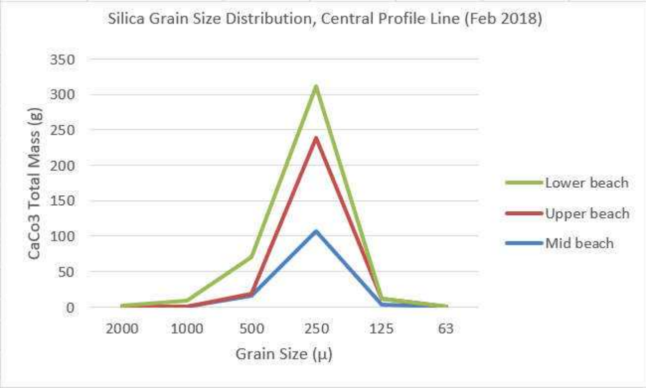

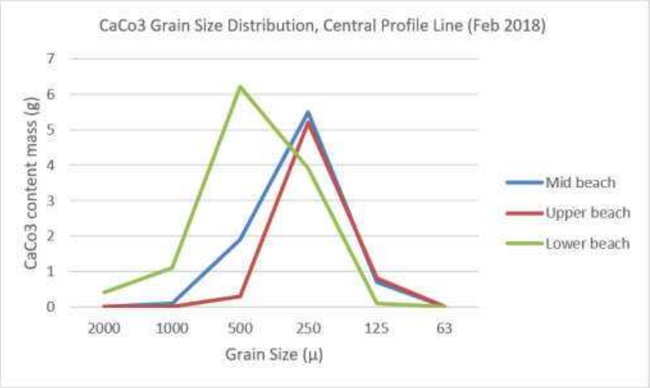

The Silica grain size distribution for the Central Profile Line for February 2018 indicate a largely homogenous size mix of 250 μ across the inshore-offshore extent of the beach. The CaCo3 composition of the sand at that time on 2nd Beach was a low 5.2 % by mass of the total sample mass. The Lower Beach (closest to the water line) exhibited the largest CaCo3 grain size peak of 500 μ. This is shown as a green line in the Right-Hand side graph plot. The grain size distribution plots above are shown here for the Central Profile Line only for February 2018.

Waves

Although Waves as a topic was not defined in the call for proposals originally, it was decided to nevertheless include it here for completeness and its significant contribution to the physical dynamics of the site.

Geospatial setting

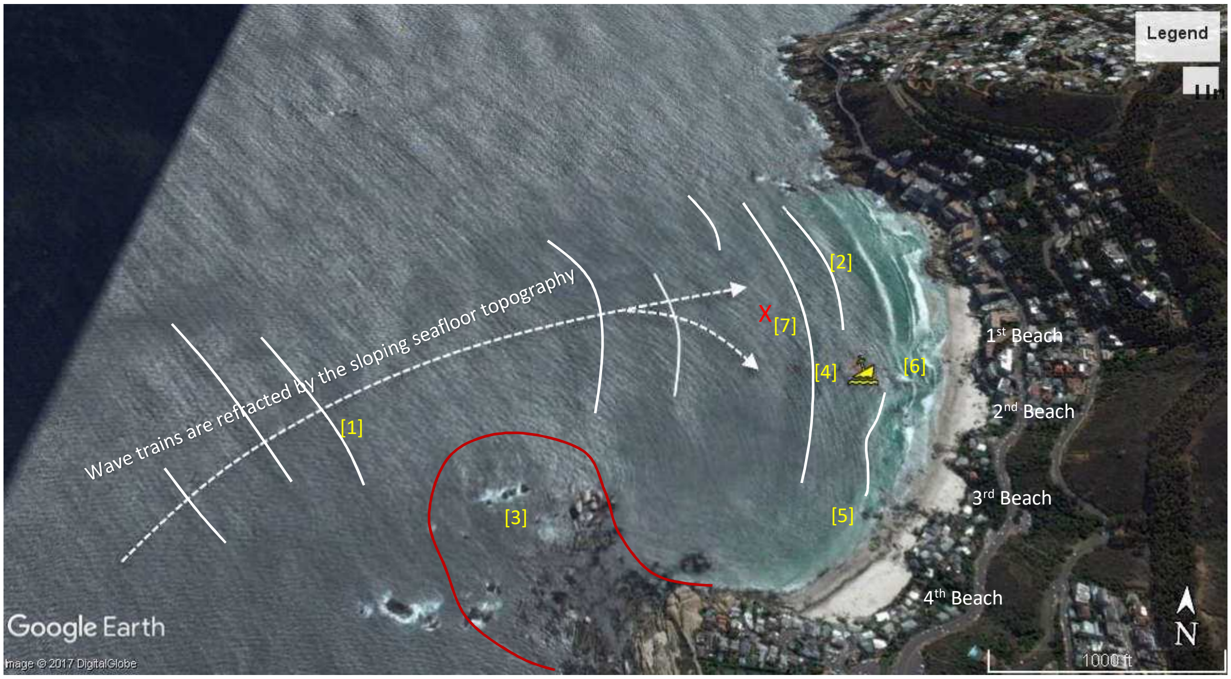

The Google image above, provides a useful representation of the complex wave field of Clifton Bay. In the image the “year-round” prevailing southwesterly swell can be seen impacting the sloping the northern sector (1st Beach) as it travels in wave so-called “trains” [1] before breaking in the surf zone [2]. The protection offered by the rocky outcrop in the southern part of Clifton Bay [3] is clearly visible as the waves are seen to refract from southwesterly to westerly direction [4] at second and third beach. The waves at 4th Beach are only exposed to northwesterly swells and hence are completely protected by the outcrop, reducing the wave impact (wave height and energy) there significantly [5].

The reefs at the wreck site in the middle of the bay can be seen refracting and dissipating the wave energy, creating a complex energetic region between the wreck site and the inter-tidal zone [6]. The consequence of this raised wave energy pocket is increased stream flow over the wreck site. Such conditions likely contribute the formation of strong turbulent slip currents at boundary interfaces such as the reef where the *São José* wrecked. These slip currents bring with them increased exposure of the wreck site to well-mixed and well oxygenated water (from the intertidal zone) as it flows offshore, past and between the wreck site reefs. The Acoustic Doppler Current Profiler, which also recorded wave information was deployed at the location denoted with an “X” [7]. An extract from the time series of the wave and current data are provided below. The volume of completed dataset recorded in each instance is too large for this report.

Times Series records

Analysis of the data for this aspect of the project is a complex and extensive exercise and is expected to be completed at a later stage. However, exerts or “snap shots” of the results are provided below for a 20 minute interval at 12h00 for the first 4 days of the deployment.

Winter Waves Conditions

Winter wave conditions are shown in the images below for the first 4 days of the deployment.

10(12h00) -11(12h00) July 2018

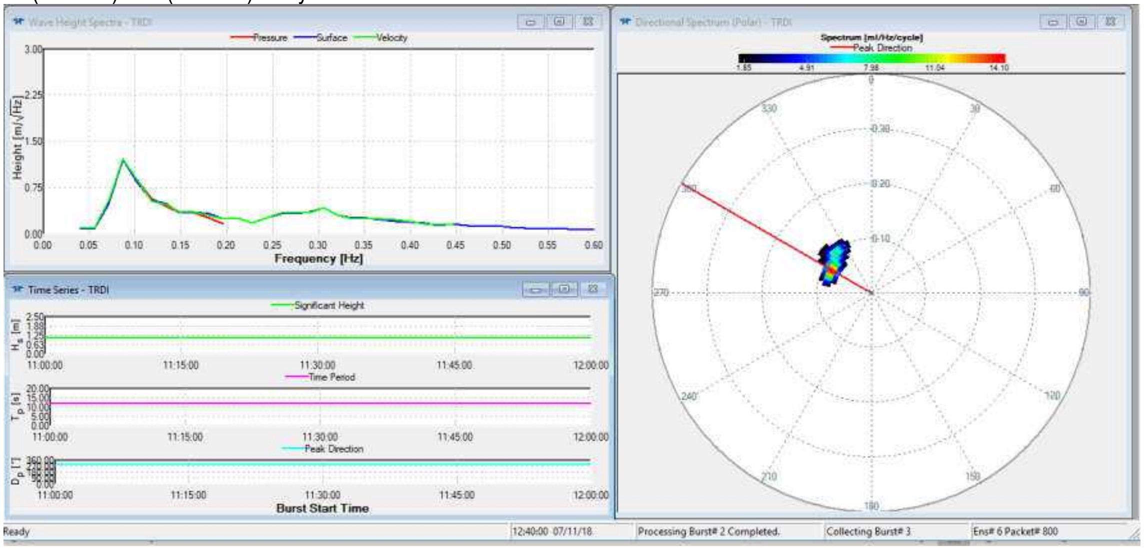

Ready | 12:40:00 07/11/18 | Processing Burst# 2 Completed. | Collecting Burst# 3 | Ens# 6 Packet# 800

11(12h00) -12(12h00) July 2018

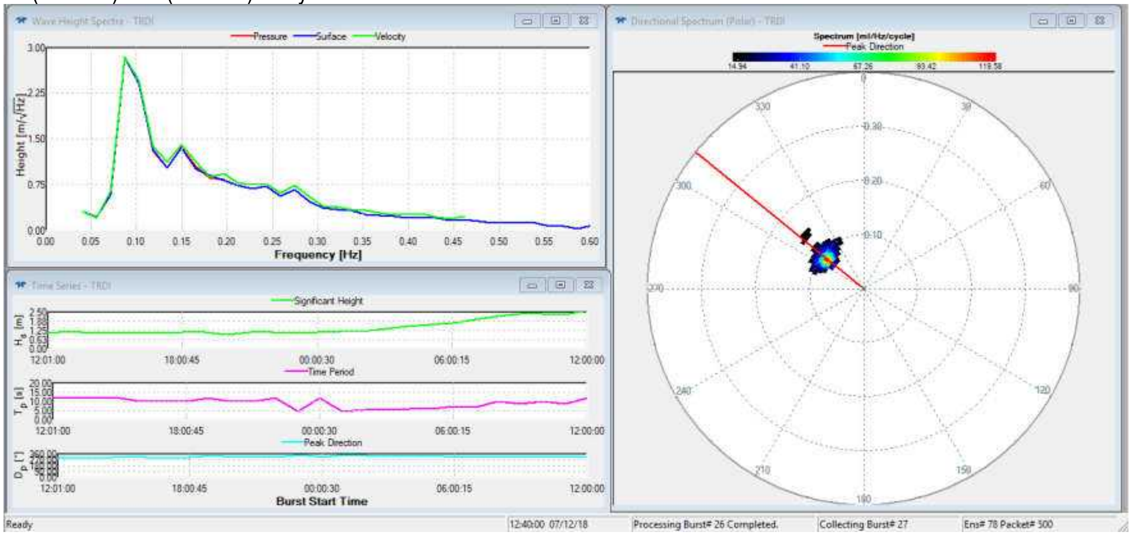

Ready | 12:40:00 07/12/18 | Processing Burst# 26 Completed. | Collecting Burst# 27 | Ens# 78 Packet# 500

12(12h00) -13(12h00) July 2018

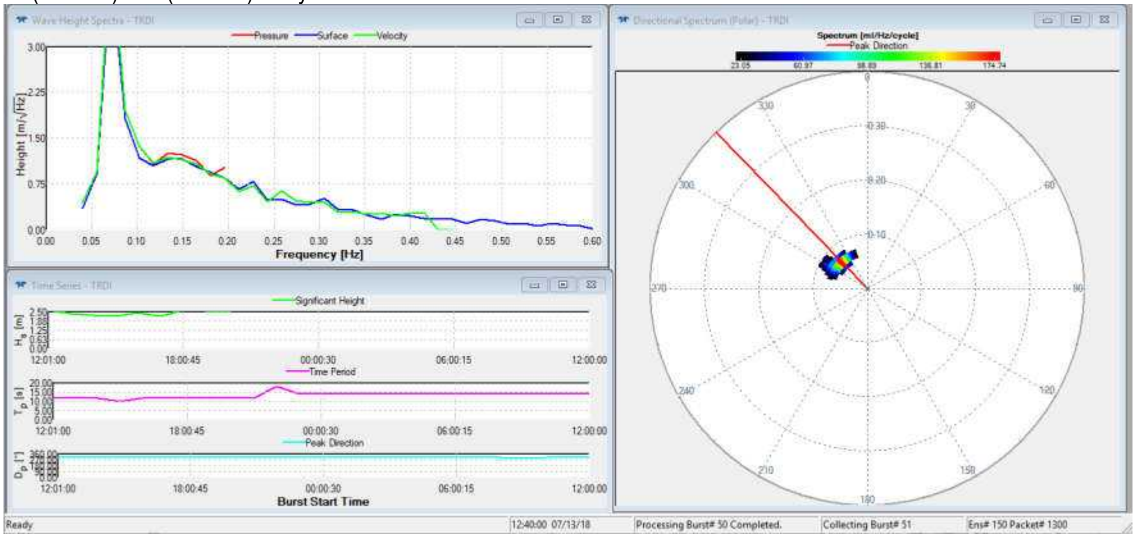

Ready

12:40:00 07/13/18

Processing Burst# 50 Completed.

Collecting Burst# 51

Ens# 150 Packet# 1300

13(12h00) -14(12h00) July 2018

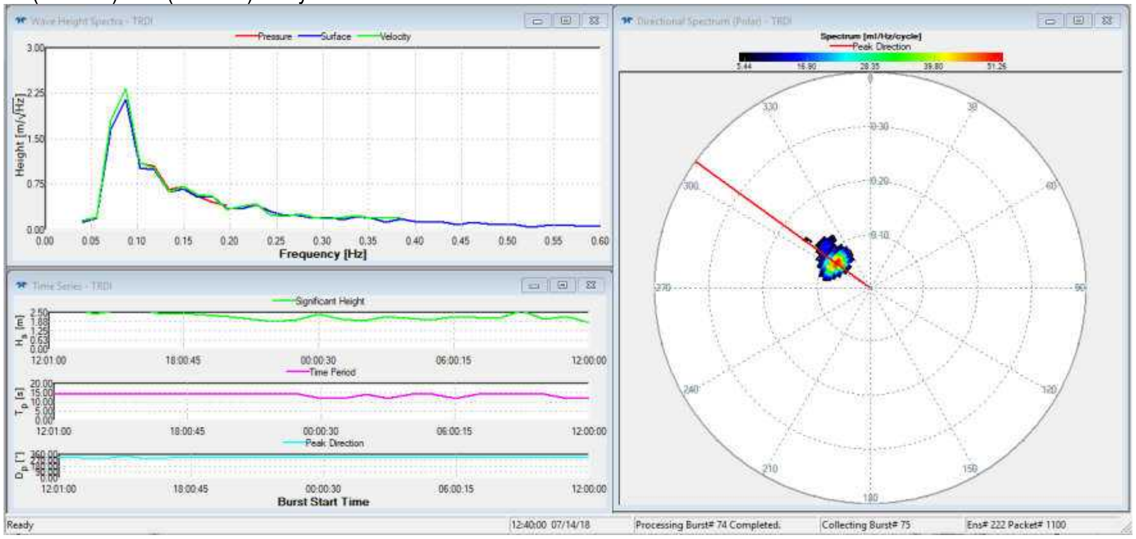

Ready

12:40:00 07/14/18

Processing Burst# 74 Completed.

Collecting Burst# 75

Ens# 222 Packet# 1100

Summer Wave Conditions

Summer wave conditions are shown in the images below for the first 4 days of the deployment.

28(11h55) -29(11h55) November 2018

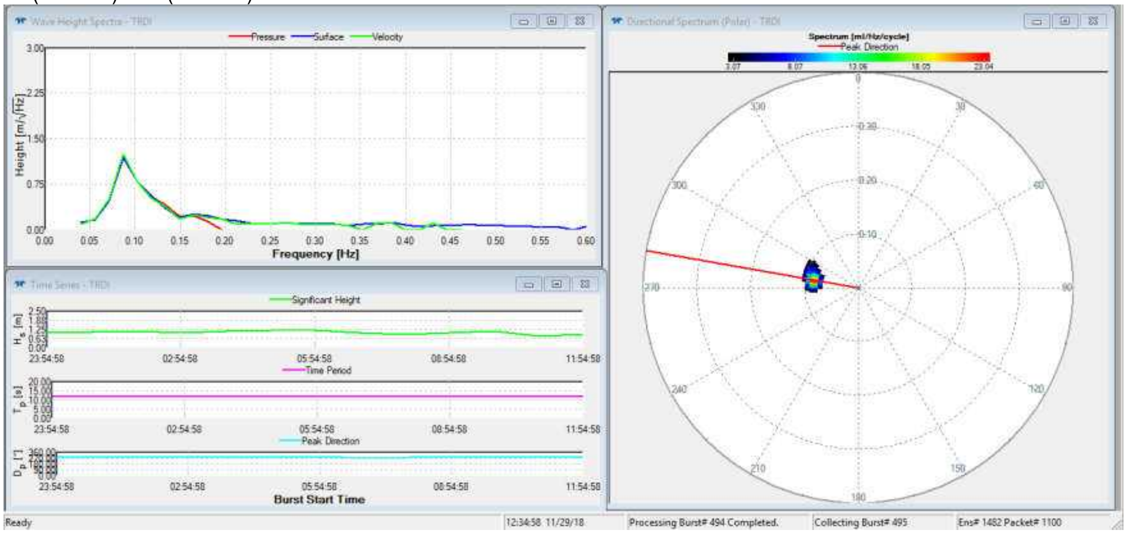

Ready | 12:34:58 11/29/18 | Processing Burst# 494 Completed. | Collecting Burst# 495 | Ens# 1482 Packet# 1100

29(11h55) -30(11h55) November 2018

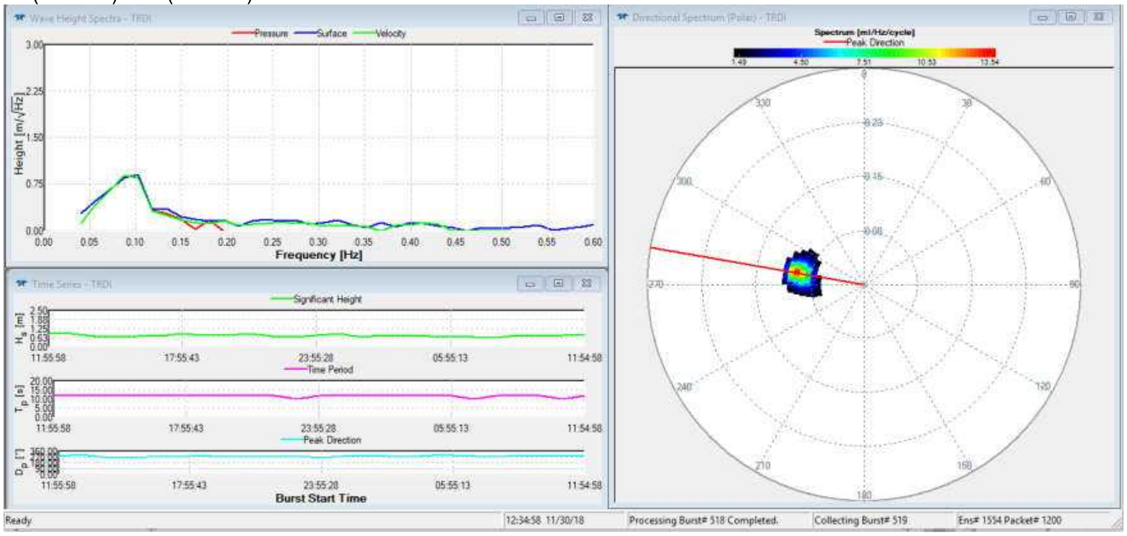

Ready | 12:34:58 11/30/18 | Processing Burst# 518 Completed. | Collecting Burst# 519 | Ens# 1554 Packet# 1200

30 November (11h55) – 1 December (11h55) 2018

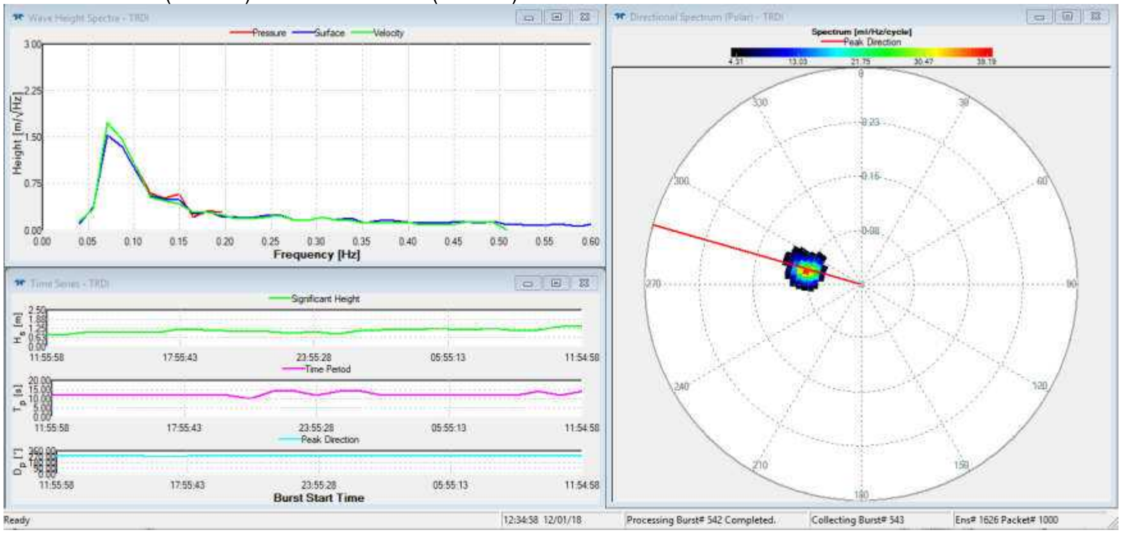

Ready 12:34:58 12/01/18 Processing Burst# 542 Completed. Collecting Burst# 543 Ens# 1626 Packet# 1000

1(11h55) – 2 December (11h55) 2018

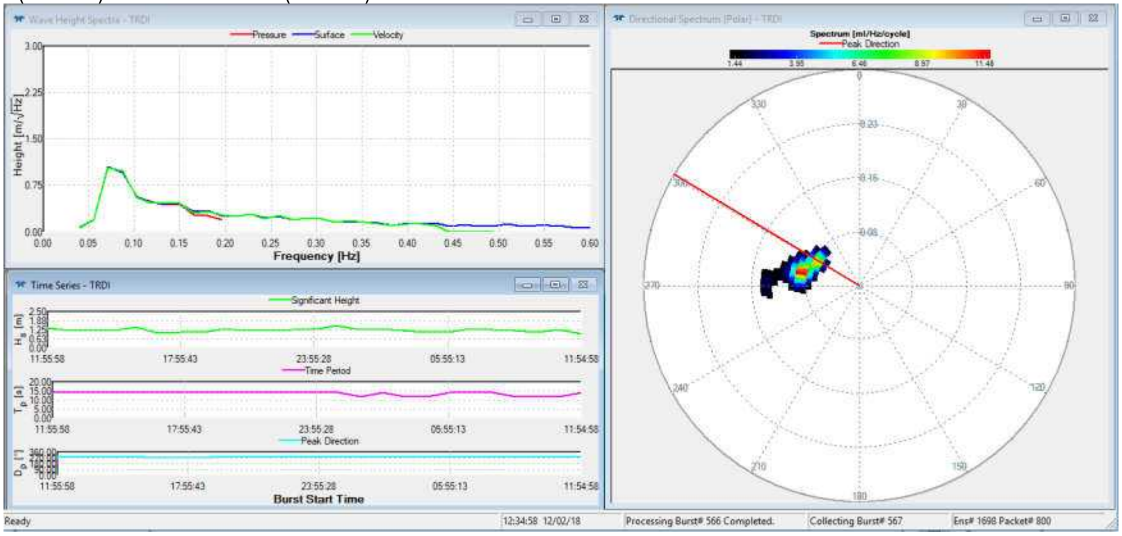

Ready 12:34:58 12/02/18 Processing Burst# 566 Completed. Collecting Burst# 567 Ens# 1698 Packet# 800

Currents

An Acoustic Doppler Current (ADCP) profiler was deployed at the location shown above in the Geospatial Setting section of this document. The instrument measured currents as well as waves.

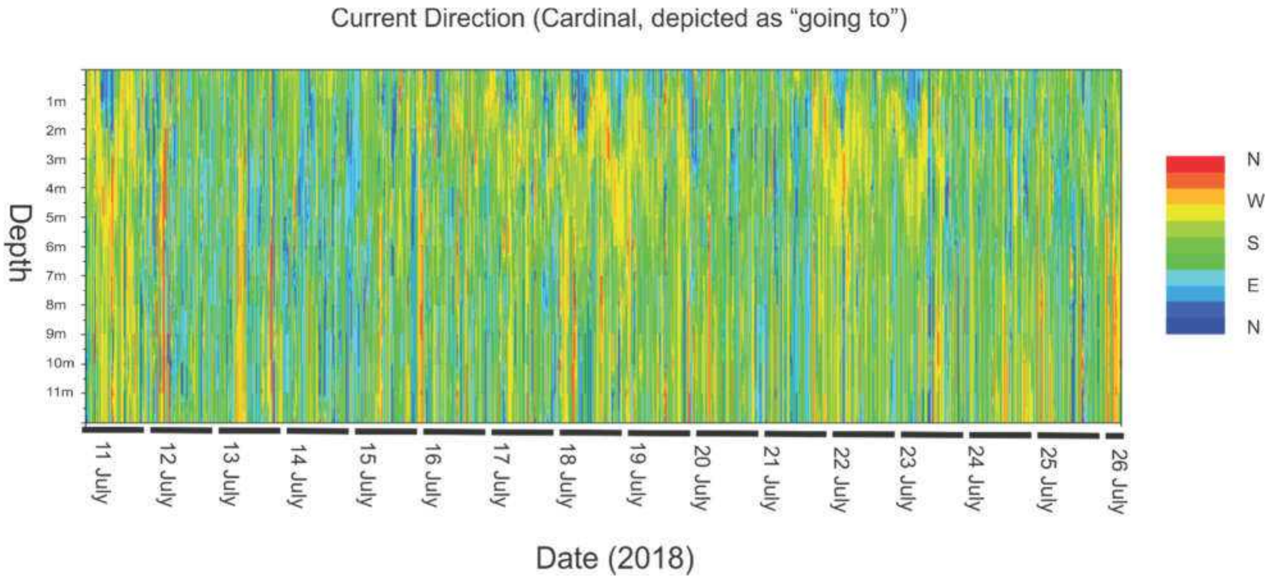

Tides are one of the important driving forces of coastal currents. The predicted tides are generated by the SA Hydrographic Office are provided here for July – September 2018 for the nearby port of Cape Town.

CAPE TOWN

2018

TIME ZONE - 2

TIME ZONE - 2

JULY						AUGUST						SEPTEMBER					
DAY	TIME	M	DAY	TIME	M	DAY	TIME	M	DAY	TIME	M	DAY	TIME	M	DAY	TIME	M
1	04 53	1.50	16	05 37	1.68	1	05 39	1.49	16	00 42	0.37	1	00 26	0.44	16	01 26	0.62
S	11 02	0.38	M	11 46	0.21	W	11 43	0.40	T	06 43	1.48	S	06 30	1.43	$	07 42	1.25
	17 21	1.53		18 02	1.75		18 05	1.56		12 44	0.43		12 29	0.51		13 42	0.72
	23 25	0.47								19 03	1.56		18 54	1.50		19 58	1.24
2	05 27	1.46	17	00 24	0.31	2	00 15	0.47	17	01 31	0.50	2	01 15	0.51	17	02 34	0.72
M	11 35	0.42	T	06 26	1.57	T	06 16	1.44	F	07 32	1.35	$	07 21	1.34	M	09 06	1.16
	17 57	1.49		12 33	0.31		12 18	0.47		13 32	0.58		13 22	0.61		15 19	0.81
				18 52	1.66		18 44	1.51		19 54	1.42		19 51	1.40	◑	21 33	1.15
3	00 03	0.51	18	01 19	0.40	3	00 59	0.52	18	02 29	0.62	3	02 21	0.59	18	04 26	0.76
T	06 04	1.40	W	07 18	1.45	F	06 59	1.37	S	08 35	1.23	M	08 33	1.26	T	10 58	1.17
	12 11	0.48		13 23	0.44		13 01	0.54		14 36	0.70		14 43	0.69		17 17	0.79
	18 36	1.45		19 45	1.55		19 30	1.45	◑	20 59	1.29	◐	21 14	1.33		23 22	1.17
4	00 47	0.56	19	02 19	0.50	4	01 52	0.57	19	03 48	0.69	4	03 53	0.62	19	05 57	0.71
W	06 45	1.34	T	08 17	1.33	S	07 54	1.30	$	10 03	1.17	T	10 13	1.25	W	12 14	1.25
	12 52	0.54		14 21	0.56		13 56	0.62		16 11	0.77		16 35	0.69		18 27	0.70
	19 22	1.41	◑	20 45	1.45	◐	20 30	1.40		22 27	1.23		22 51	1.35			
5	01 39	0.61	20	03 27	0.58	5	03 01	0.60	20	05 19	0.69	5	05 26	0.56	20	00 30	1.25
T	07 36	1.28	F	09 28	1.25	$	09 07	1.25	M	11 36	1.20	W	11 44	1.34	T	06 50	0.61
	13 43	0.60		15 32	0.65		15 14	0.68		17 46	0.75		18 04	0.59		13 01	1.36
	20 17	1.38		21 55	1.37		21 45	1.38		23 51	1.25					19 09	0.60
6	02 41	0.63	21	04 43	0.62	6	04 22	0.59	21	06 30	0.64	6	00 11	1.44	21	01 14	1.35
F	08 40	1.24	S	10 48	1.23	M	10 35	1.26	T	12 42	1.28	T	06 36	0.44	F	07 27	0.52
	14 48	0.65		16 53	0.70		16 47	0.66		18 49	0.68		12 50	1.49		13 37	1.46
◐	21 23	1.37		23 08	1.34		23 06	1.41					19 07	0.44		19 43	0.49
7	03 53	0.61	22	05 54	0.60	7	05 41	0.51	22	00 51	1.31	7	01 12	1.57	22	01 49	1.45
S	09 57	1.24	$	12 03	1.26	T	11 56	1.35	W	07 17	0.56	F	07 30	0.31	S	07 57	0.43
	16 05	0.66		18 07	0.68		18 08	0.58		13 28	1.37		13 42	1.65		14 08	1.56
	22 32	1.41								19 32	0.59		19 57	0.29		20 13	0.40
8	05 04	0.55	23	00 13	1.35	8	00 17	1.49	23	01 35	1.39	8	02 04	1.69	23	02 20	1.54
$	11 13	1.29	M	06 51	0.55	W	06 47	0.40	T	07 53	0.48	S	08 16	0.19	$	08 25	0.35
	17 20	0.62		13 00	1.33		12 59	1.47		14 04	1.46		14 27	1.79		14 37	1.65
	23 36	1.47		19 03	0.63		19 11	0.45		20 07	0.50		20 43	0.17		20 42	0.33
9	06 07	0.46	24	01 06	1.39	9	01 18	1.60	24	02 11	1.47	9	02 49	1.78	24	02 49	1.61
M	12 18	1.39	T	07 35	0.49	T	07 41	0.28	F	08 24	0.40	$	08 57	0.12	M	08 53	0.30
	18 24	0.53		13 45	1.40		13 54	1.61		14 35	1.54		15 10	1.88		15 05	1.71
				19 47	0.56		20 05	0.32		20 37	0.43	●	21 25	0.11		21 11	0.27
10	00 35	1.56	25	01 49	1.44	10	02 12	1.70	25	02 43	1.53	10	03 32	1.82	25	03 18	1.65
T	07 02	0.35	W	08 12	0.44	F	08 30	0.18	S	08 53	0.34	M	09 37	0.09	T	09 20	0.26
	13 14	1.50		14 22	1.47		14 42	1.74		15 05	1.61		15 50	1.92		15 34	1.76
	19 20	0.43		20 23	0.50		20 54	0.21		21 07	0.37		22 06	0.10	○	21 41	0.23
11	01 29	1.65	26	02 26	1.48	11	03 02	1.78	26	03 13	1.58	11	04 12	1.80	26	03 48	1.68
W	07 53	0.25	T	08 44	0.39	S	09 15	0.10	$	09 20	0.30	T	10 15	0.12	W	09 49	0.25
	14 05	1.61		14 56	1.53		15 28	1.84		15 34	1.66		16 29	1.90		16 03	1.78
	20 12	0.33		20 56	0.45	●	21 41	0.15	○	21 36	0.33		22 46	0.14		22 12	0.22
12	02 21	1.73	27	03 01	1.53	12	03 49	1.81	27	03 43	1.62	12	04 51	1.74	27	04 19	1.68
T	08 41	0.16	F	09 13	0.35	$	09 58	0.08	M	09 47	0.28	W	10 52	0.19	T	10 19	0.27
	14 54	1.71		15 27	1.57		16 12	1.88		16 03	1.70		17 07	1.82		16 34	1.76
	21 02	0.25	○	21 27	0.41		22 27	0.13		22 06	0.30		23 24	0.24		22 45	0.24
13	03 11	1.78	28	03 33	1.55	13	04 33	1.79	28	04 12	1.63	13	05 30	1.63	28	04 52	1.64
F	09 28	0.11	S	09 42	0.32	M	10 40	0.10	T	10 15	0.27	T	11 29	0.31	F	10 51	0.32
	15 41	1.78		15 58	1.60		16 55	1.88		16 32	1.71		17 43	1.70		17 08	1.71
●	21 52	0.20		21 58	0.39		23 12	0.17		22 38	0.30					23 21	0.29
14	04 00	1.79	29	04 04	1.57	14	05 16	1.72	29	04 42	1.61	14	00 02	0.36	29	05 28	1.58
S	10 14	0.10	$	10 11	0.31	T	11 21	0.18	W	10 44	0.30	F	06 08	1.51	S	11 27	0.39
	16 28	1.81		16 28	1.62		17 37	1.81		17 02	1.69		12 06	0.45		17 45	1.62
	22 41	0.19		22 30	0.38		23 57	0.26		23 10	0.33		18 21	1.54			
15	04 49	1.76	30	04 34	1.56	15	05 59	1.61	30	05 14	1.58	15	00 41	0.49	30	00 01	0.37
$	10 59	0.13	M	10 40	0.32	W	12 02	0.29	T	11 15	0.34	S	06 50	1.37	$	06 10	1.49
	17 15	1.80		16 59	1.62		18 19	1.70		17 35	1.65		12 47	0.59		12 10	0.50
	23 32	0.23		23 02	0.40					23 46	0.37		19 02	1.38		18 30	1.50
			31	05 06	1.54				31	05 49	1.52						
			T	11 10	0.35				F	11 49	0.42						
				17 31	1.60					18 11	1.58						
				23 37	0.43												

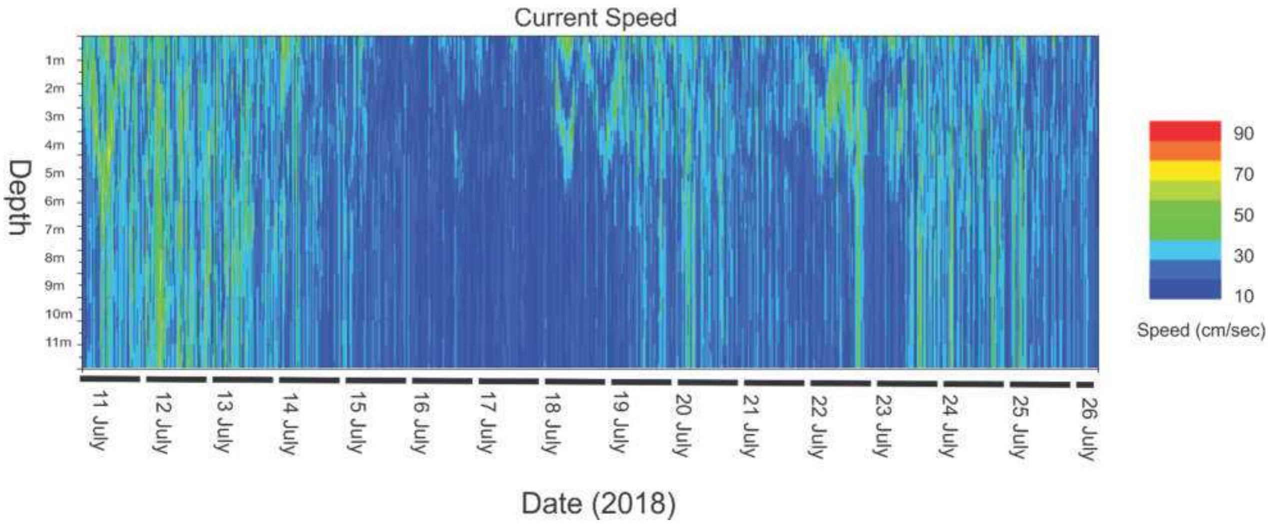

Summer Current profiles

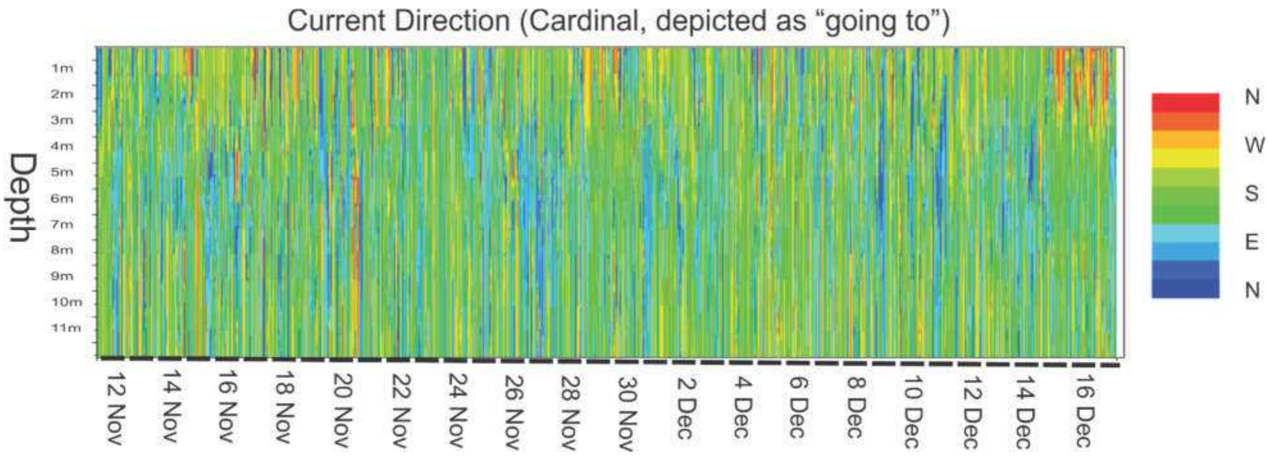

Tides are one of the important driving forces of coastal currents. The predicted tides are generated by the SA Hydrographic Office are provided here for July – September 2018 for the nearby port of Cape Town.

CAPE TOWN

2018

TIME ZONE - 2

TIME ZONE - 2

OCTOBER						NOVEMBER						DECEMBER					
DAY	TIME	M	DAY	TIME	M	DAY	TIME	M	DAY	TIME	M	DAY	TIME	M	DAY	TIME	M
1 M	00 50 07 01 13 07 19 30	0.48 1.38 0.61 1.38	16 T ◑	01 27 08 07 14 22 20 26	0.70 1.20 0.80 1.13	1 T	03 20 09 48 16 30 22 33	0.62 1.35 0.63 1.30	16 F	03 25 10 12 16 38 22 42	0.76 1.25 0.75 1.17	1 S	04 17 10 41 17 23 23 24	0.60 1.48 0.53 1.35	16 $	03 22 10 03 16 33 22 35	0.74 1.34 0.70 1.21
2 T ◐	01 57 08 17 14 39 21 01	0.58 1.29 0.70 1.29	17 W	03 02 09 56 16 22 22 28	0.77 1.17 0.81 1.12	2 F	04 52 11 13 17 48 23 50	0.59 1.44 0.52 1.39	17 S	04 56 11 22 17 43 23 49	0.73 1.33 0.66 1.25	2 $	05 30 11 46 18 23	0.57 1.54 0.45	17 M	04 42 11 08 17 37 23 44	0.72 1.40 0.62 1.29
3 W	03 36 10 02 16 37 22 45	0.64 1.28 0.68 1.31	18 T	04 58 11 26 17 45 23 51	0.76 1.24 0.72 1.20	3 S	06 01 12 15 18 44	0.50 1.56 0.40	18 $	05 55 12 10 18 29	0.65 1.43 0.55	3 M	00 26 06 29 12 39 19 12	1.43 0.51 1.61 0.38	18 T	05 46 12 01 18 28	0.66 1.48 0.51
4 T	05 14 11 33 18 01	0.58 1.38 0.55	19 F	06 06 12 20 18 34	0.67 1.34 0.62	4 $	00 47 06 53 13 04 19 30	1.50 0.41 1.67 0.29	19 M	00 37 06 39 12 50 19 07	1.35 0.57 1.53 0.44	4 T	01 16 07 17 13 24 19 53	1.50 0.46 1.66 0.32	19 W	00 37 06 38 12 48 19 12	1.39 0.58 1.58 0.40
5 F	00 05 06 23 12 36 18 59	1.42 0.47 1.53 0.40	20 S	00 40 06 48 12 59 19 10	1.31 0.58 1.45 0.51	5 M	01 34 07 37 13 46 20 10	1.60 0.33 1.76 0.21	20 T	01 15 07 16 13 26 19 42	1.46 0.48 1.63 0.33	5 W	01 59 07 59 14 05 20 30	1.57 0.42 1.69 0.28	20 T	01 22 07 23 13 32 19 54	1.50 0.48 1.67 0.29
6 S	01 03 07 14 13 25 19 46	1.55 0.34 1.68 0.26	21 $	01 17 07 22 13 32 19 42	1.42 0.48 1.56 0.40	6 T	02 15 08 16 14 25 20 47	1.67 0.28 1.81 0.17	21 W	01 51 07 51 14 01 20 17	1.56 0.40 1.72 0.24	6 T	02 38 08 37 14 43 21 04	1.62 0.39 1.69 0.27	21 F	02 05 08 07 14 15 20 35	1.60 0.40 1.75 0.20
7 $	01 51 07 57 14 08 20 27	1.66 0.24 1.80 0.16	22 M	01 50 07 53 14 03 20 13	1.51 0.40 1.66 0.31	7 W ●	02 54 08 53 15 02 21 21	1.70 0.26 1.81 0.17	22 T	02 27 08 27 14 36 20 53	1.64 0.33 1.78 0.17	7 F ●	03 15 09 13 15 18 21 36	1.64 0.39 1.67 0.28	22 S ○	02 47 08 50 14 59 21 18	1.69 0.33 1.80 0.15
8 M	02 33 08 37 14 48 21 06	1.74 0.17 1.88 0.11	23 T	02 21 08 22 14 33 20 44	1.60 0.33 1.74 0.23	8 T	03 30 09 28 15 37 21 54	1.71 0.28 1.77 0.21	23 F ○	03 04 09 04 15 14 21 30	1.70 0.29 1.81 0.14	8 S	03 49 09 47 15 52 22 07	1.64 0.41 1.63 0.31	23 $	03 30 09 36 15 45 22 01	1.75 0.28 1.81 0.13
9 T ●	03 12 09 14 15 25 21 43	1.78 0.15 1.90 0.11	24 W ○	02 52 08 52 15 04 21 15	1.66 0.28 1.79 0.18	9 F	04 05 10 02 16 10 22 26	1.68 0.33 1.70 0.27	24 S	03 42 09 44 15 54 22 10	1.73 0.28 1.80 0.15	9 $	04 22 10 21 16 25 22 37	1.62 0.44 1.58 0.35	24 M	04 15 10 23 16 32 22 46	1.78 0.27 1.78 0.16
10 W	03 50 09 50 16 01 22 19	1.77 0.18 1.86 0.16	25 T	03 24 09 24 15 36 21 49	1.70 0.26 1.81 0.16	10 S	04 39 10 36 16 43 22 57	1.62 0.40 1.60 0.35	25 $	04 23 10 26 16 37 22 53	1.73 0.31 1.75 0.20	10 M	04 56 10 55 16 58 23 08	1.58 0.48 1.52 0.41	25 T	05 01 11 13 17 20 23 33	1.78 0.30 1.72 0.23
11 T	04 26 10 25 16 36 22 52	1.72 0.25 1.78 0.24	26 F	03 58 09 58 16 11 22 24	1.71 0.27 1.79 0.18	11 $	05 13 11 11 17 16 23 28	1.55 0.49 1.50 0.44	26 M	05 07 11 14 17 24 23 40	1.69 0.37 1.65 0.29	11 T	05 29 11 30 17 32 23 41	1.53 0.54 1.44 0.47	26 W	05 50 12 07 18 12	1.74 0.37 1.62
12 F	05 02 10 59 17 10 23 25	1.63 0.35 1.65 0.35	27 S	04 34 10 35 16 48 23 03	1.69 0.31 1.73 0.24	12 M	05 49 11 48 17 52	1.46 0.58 1.38	27 T	05 55 12 09 18 17	1.62 0.45 1.54	12 W	06 06 12 10 18 09	1.47 0.60 1.36	27 T	00 23 06 42 13 06 19 08	0.32 1.67 0.45 1.50
13 S	05 37 11 34 17 44 23 58	1.52 0.47 1.51 0.47	28 $	05 14 11 16 17 30 23 46	1.63 0.39 1.63 0.33	13 T	00 03 06 29 12 33 18 33	0.54 1.37 0.67 1.28	28 W	00 33 06 52 13 15 19 21	0.40 1.54 0.54 1.41	13 T	00 18 06 48 12 58 18 54	0.55 1.40 0.67 1.29	28 F	01 17 07 40 14 13 20 12	0.43 1.59 0.53 1.39
14 $	06 14 12 12 18 20	1.41 0.59 1.37	29 M	05 59 12 05 18 20	1.54 0.49 1.50	14 W	00 46 07 22 13 35 19 32	0.63 1.28 0.75 1.18	29 T	01 36 08 02 14 37 20 40	0.50 1.47 0.60 1.33	14 F	01 03 07 41 13 59 19 52	0.63 1.35 0.72 1.22	29 S ◐	02 20 08 47 15 29 21 27	0.54 1.52 0.58 1.31
15 M	00 35 06 59 13 01 19 06	0.59 1.29 0.71 1.23	30 T	00 38 06 55 13 11 19 25	0.45 1.43 0.60 1.37	15 T ◑	01 49 08 40 15 05 21 04	0.72 1.23 0.79 1.13	30 F ◐	02 54 09 22 16 06 22 07	0.58 1.44 0.59 1.31	15 S ◑	02 03 08 49 15 15 21 11	0.70 1.32 0.74 1.19	30 $	03 34 09 59 16 48 22 48	0.62 1.48 0.59 1.30
			31 W ◐	01 47 08 12 14 45 20 55	0.56 1.35 0.66 1.29										31 M	04 53 11 11 17 58	0.65 1.48 0.55

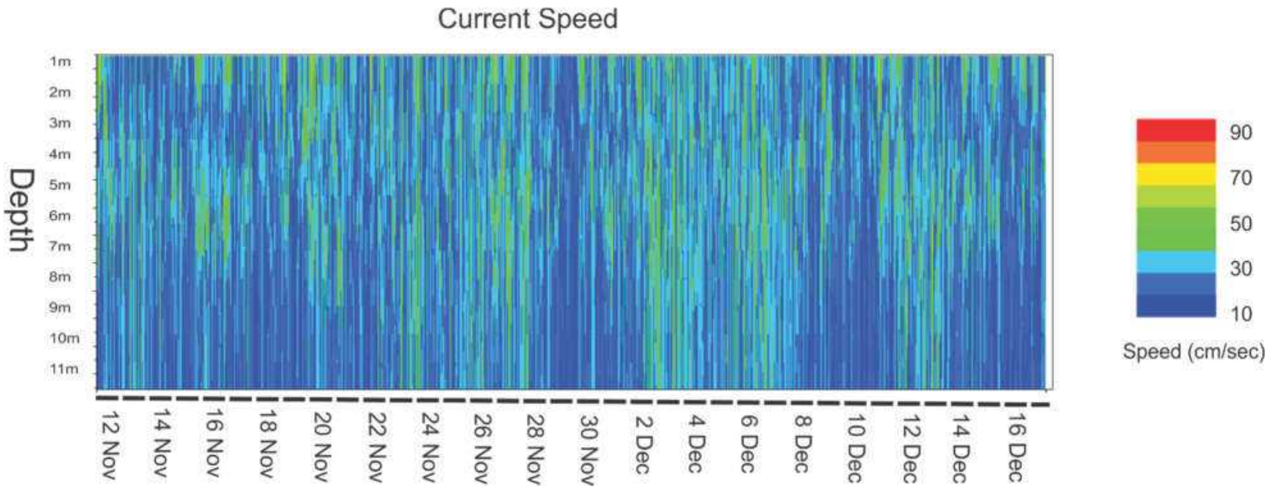

Water Properties

Dissolved Oxygen and Temperature

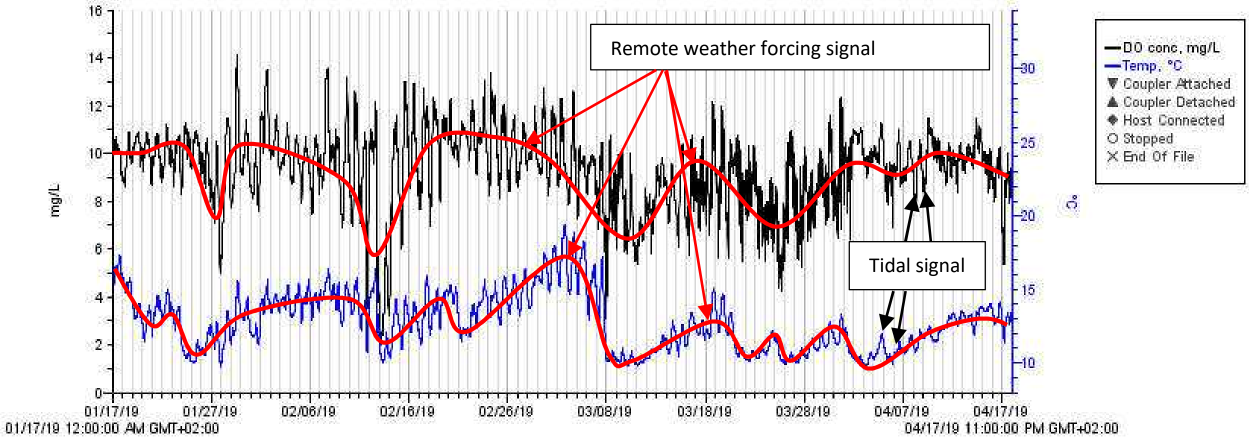

A Hobo Dissolved Oxygen Logger was deployed at one of the datum points on the wreck site, by attaching the instrument to an eye bolt inserted into the reef. The logger was set to a sampling interval of 15 minutes and recorded temperature and dissolved oxygen. The record started on 17 January 2019 and ended on 17 April 2019. Each day is shown on the x-axis as a vertical grey line in the plot above.

Although detailed analysis of the data is still required, two features (a high frequency and low frequency signal) appear to dominate both the dissolved oxygen and the temperature time series records. The high frequency signal seen here as a noisy daily fluctuation, is attributed to tides and can be seen in the expanded plot below. The lower frequency or longer-term fluctuations in the signal may be attributed to remote forcing effects of weather or swell events. The temperature and dissolved oxygen plots are roughly coincident with each other.

Conductivity and Temperature

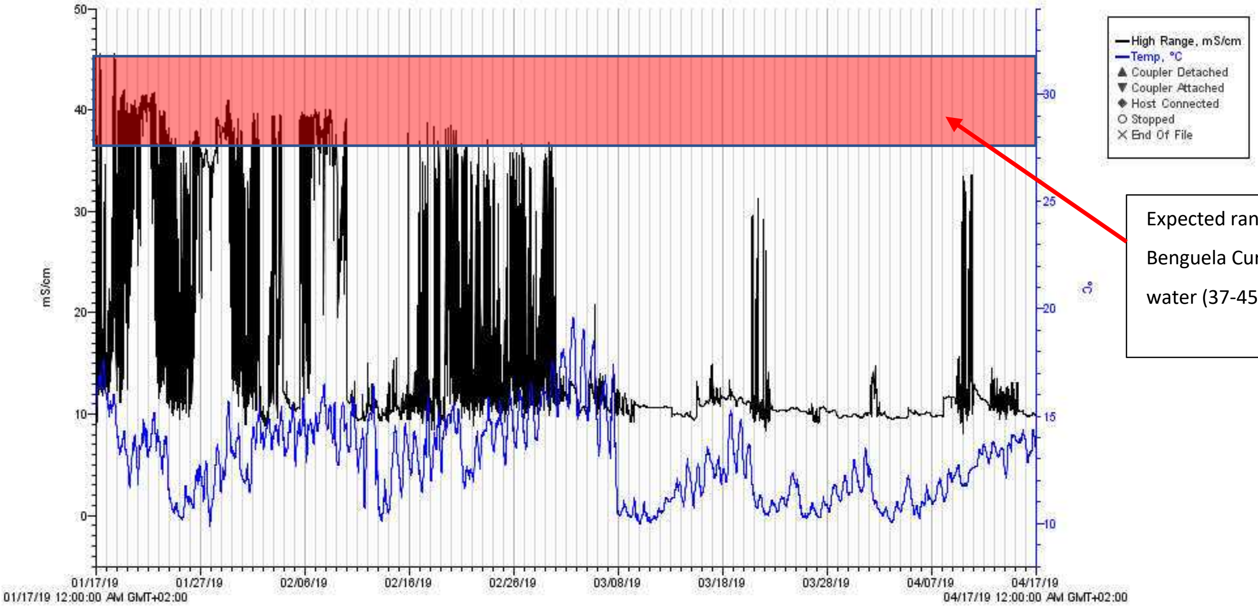

Expected range for Benguela Current water (37-45 mS)

A Hobo High Range Conductivity Logger was deployed at the same datum point location as the Dissolved Oxygen Logger above. The same method of attachment of the instrument to an eye bolt inserted into the reef was used. The logger was set to a sampling interval of 15 minutes and recorded temperature and dissolved oxygen. The record started on 17 January 2019 and ended on 17 April 2019. Each day is shown on the x-axis as a vertical grey line in the plot above.

The low overall conductivity values seen is lower than the expected conductivity for this ocean which should be between 37 and 45 mS. If the sensor is determined to be functional then the only explanation for these lower readings would be the presence groundwater flow permeating from the surrounding Table Mountain. We sent the sensor back to the supplier for maintenance. The supplier assured us that the sensor was in good working order. We, therefore, re-deployed the sensor on 4 February and recovered it a month later at the beginning of March 2020. This time the sensor seemed to have recorded the full period of deployment. There is a possibility that the first deployment was done incorrectly as we changed the location of the sensor slightly with the second deployment.

The graph below show the conductivity and temperature ranges. The sensor was set to record a reading every 30 min giving 48 readings per day. The conductivity and temperature are displayed horizontally and seems to compare favorably with the smaller Micro-CTD.

The salinity values seem to be similar to the ones previously reported are lower than expected for this general area. As this is a different sensor than the Micro-CTD, but measuring the same parameter we have to tentatively conclude that the small section of Clifton we are studying, has a lower salinity than the greater Table Bay area. We do however need to do more deployments as well as get more opinions from other scientists to conclude this observation definitively. We have however been prevented by the lockdown in deploying the sensors. The situation seems to be improving and we hope to be back on site in the near future.

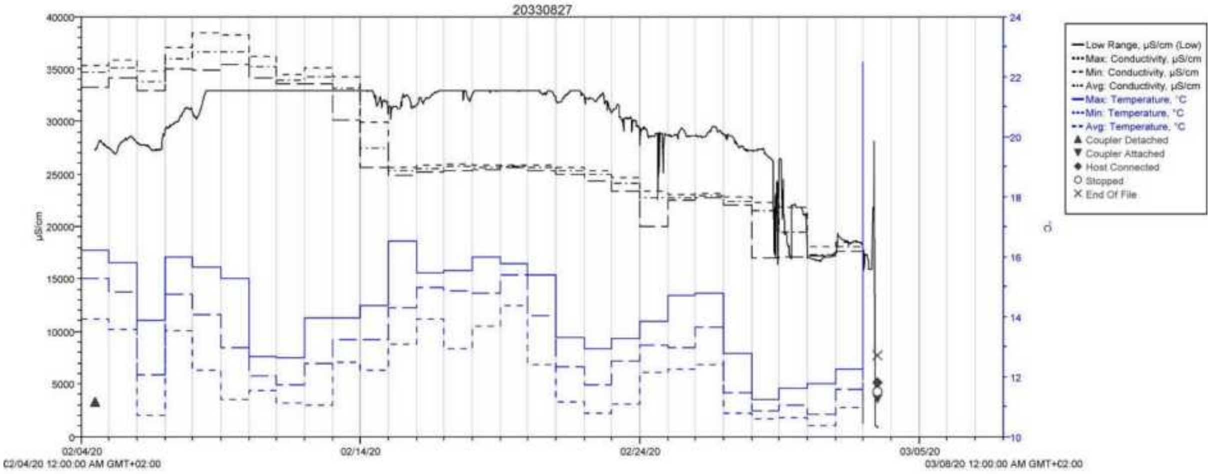

Marine Biology

(This section has been contributed.by Dr Wayne K. Florence, Curator of Marine Invertebrates – Iziko Museums.)

In addition to archaeological examination, the understanding of associated marine biodiversity is critical to the effective conservation of underwater cultural heritage. While there are a number of global studies which take this approach, (Bethencourt *et al.,* 2018; Caporaso *et al.,* 2018; Hamdan *et al*., 2018) there has been no such work performed on submerged historical shipwrecks found in South African waters. The dynamics of the interaction between historical shipwrecks and local biodiversity is therefore unknown. We have no information on the effects of colonization on the wreck artefacts themselves and our understanding of the effects of the artefacts on the local biodiversity is poor. Our inadequate multidisciplinary preparedness to manage historical shipwrecks, could potentially risk the appropriate curation and management of the artefacts of the Slave Ship *São José*.

According to studies by Meyer *et al (*2017), 3 million shipwrecks are estimated to exist worldwide, but very few of these have been investigated for archaeology and biology. There has been significant interest in how marine invertebrates such as sessile sponges, hydroids and anemones, and motile crustaceans and echinoderms, colonies shipwrecks. Meyer *et al.,* (2017) studied eight shipwrecks that were located at a depth of 100m off the US Atlantic coast and focused on the relationship between species richness and the study area (shipwrecks), and abundance and species diversity within the study site. They also stated that shipwrecks can also be used for future studies as models of larval dispersal, connectivity and recruitment.

The current study aims to improve our knowledge of *in situ* curation of historical shipwrecks, by conducting a baseline biological assessment coupled with observations around colonizers of *São José*. This will be used to make recommendations for heritage management of the shipwreck.

The research questions include:

- Which benthic macro-invertebrates are present at the site of the *São José* wreck?
- Does the wreck of the *São José* contribute to the faunal composition of the benthic macro-invertebrate faunal assemblages at Clifton?
- Which benthic macro-invertebrate fauna show substrate preference for colonizing artefacts?

The objectives of the study are to:

1. establish a baseline of macro-invertebrates present on the wreck site;
2. analyses whether the wreck site has an effect on the localized macro-invertebrate faunal assemblages;
3. determine which macro-invertebrates have the potential to colonies the artefacts of the Slave Shipwreck *São José*

Results to date

Unfortunately the biological assessment which was meant to take place during the first quarter of 2020 could not be initiated due to the Covid-19 Pandemic and the related national lockdown regulations. Due to this the results presented below should be considered incomplete and preliminary as only Objective 3 can be commented on. The project is ongoing with a dedicated master's student, Ms Nthombifikile Nxiba, working under the supervision of Dr Wayne Florence (Curator: Marine Invertebrate Collections). Sampling and data collection is rescheduled for March-May 2021.

Faunal Colonizers

The marine organisms colonizing the artefacts of the *São José* shipwreck are interesting in that they can potentially tell us much about the effects of this artificial habitat on the ecology of the biota which inhabits it and indeed the wreck itself (e.g., mechanisms of degradation, nature of the substratum, etc.). Preliminary observations suggested that there are a number of sessile colonizers of wreck artefacts include protists like red, brown and coralline algae; indicating high primary productivity on the wreck, which is not uncharacteristic of shallow, sub tidal, environments where light is plentiful. Benthic invertebrates include several lightly calcified cnidarians, hydroids, molluscs and various encrusting organisms including barnacles, sponges, sea squirts and bryozoans. A number of these sessile invertebrates have formed concretions comprised of generations of colonies encapsulating some of the wreck artefacts. These concretions which also include multiple generations of mollusc shells and calcium carbonate skeletons of bryozoans are dominated by *Chthamalus dentatus* (the Toothed Barnacle – Fig1); a tiny shell dwelling crustacean that is identified by its six-plated shell with finger-like ridges producing its characteristic star-shaped outline. This species is commonly found in the upper intertidal zone of southeast South Africa, Namibia and Angola, but extremely rare on the west coast of South Africa. The current specimens (albeit all of them dead) were, most unusually, found sub-tidally (fully submerged). Perhaps an indication that the artificial reef structure provided by the *São José* has a potential role in the introduction of rare or foreign species to the wreck site; this can only be verified once the full biological baseline assessment of the wreck site and control is completed.

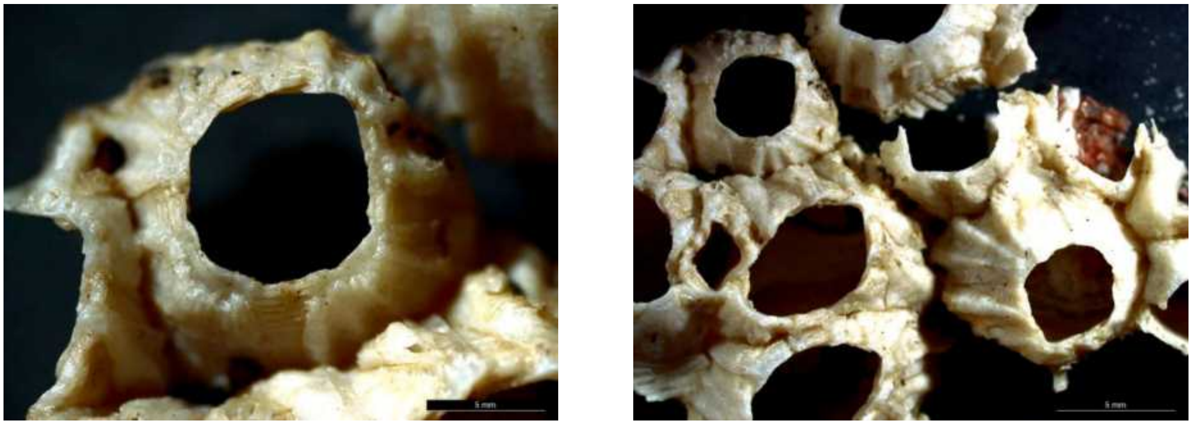

Figure 1: Dorsal view of *Chthamalus dentatus* specimens removed from a wooden artefact recovered from the *São José* wreck site

With the *São José* laying in sandy shallow sub tidal waters, the organisms living on the wreck are at least foreign to the immediate sandy bottom; a preliminary indication that the wreck objects although dispersed are promoting an artificial cold-temperate reef formation in the middle of what should be a sandy bottom. What effect that these “aliens” has in the in faunal communities of the natural sandy bottom is beyond the scope of this study but also warrants further investigation.

Substratum preference of first colonizers

The artificial sub-tidal structures created by the wreck have encouraged competition for colonization of its surfaces, which appears to be driven by substratum preference of the organisms. Understanding which taxa are first colonizers will aid in understanding what natural preservation mechanisms are acting on the *in situ São José artefacts.* Beyond the metallic objects, the artefacts recovered are mainly comprised of mangrove wood, an unknown species of *Dalbergia* (cargo wood) and *Lignum vitae* (pulley block). Settlement plates of different proxy wood types (i.e., Oak, Beech, Dalbergia, Lignum, Elm and Pine) were deployed in the wreck site to note physical wood condition following exposure. This had the incidental qualitative utility of shedding light on substrate preference of first colonizing organisms. Preliminary results suggest that the barnacle, *C. dentatus*, is the dominant faunal colonizer of the proxy submerged wood samples; competently out-competing all other macro-fauna for space on all of the samples but *Lignum* and *Dalbergia* (see figure 2a). The coralline alga, *Leptophytum* sp., dominates on all samples of *Lignum* and *Dalbergia* (see figure 2b).

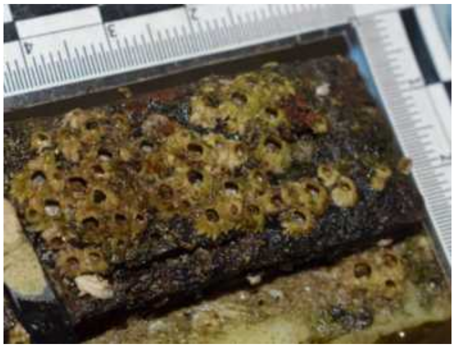

Figure 2a: Proxy wood colonized by *C. dentatus*

Figure 2b: *Dalbergia* colonized by *Leptophytum* sp

Coralline algae are a major contributor to the thick layer of concretion that has been observed on some artefacts; naturally preserving the artefacts *in situ* in an almost sealed layer. Likewise generational layers of barnacles may also contribute to concretion. The results of the wood preference of the barnacles in Figure 3 below suggests that *C. dentatus* prefers Beech and Oak wood whereas *Dalbergia* and *Lignum* is the least preferred. As mentioned above both *Dalbergia* and *Lignum* is dominated by the coralline algae, *Leptophytum* sp., which probably creates unfavorable conditions for the filter feeding barnacle and outcompetes it for space. Unfortunately we have no information of first colonizers on Mangrove.

Figure 3 - Average number of barnacles per proxy wood sample (n=2)

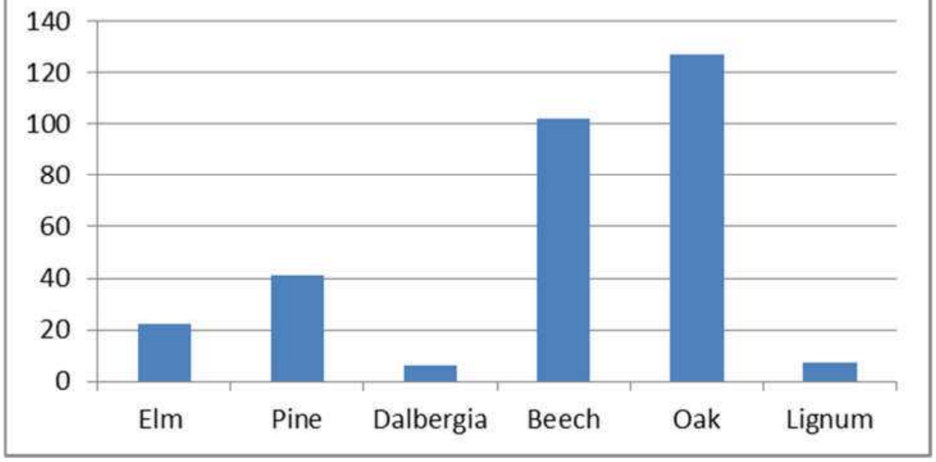

Evidence of Wood Borers

In contrast to the potential protection that colonizers may afford the wreck objects, there is evidence that animals may be boring into the wooden structures of the *São José* (see Figure 4 below).

Figure 4: Evidence of wood borer damage to an artefact recovered from the wreck of the *São José*

Just which animals are responsible for this degradation requires further investigation but the nature of the damage suggest that a boring bivalve (commonly known as a shipworm) may be resident on the wreck. From Iziko's significant species occurrence databases and associated annals we are able to establish that at least two species of shipworm, *Bankia martensi* and *Bankia carinata*, are present along the west coast of South Africa and Namibia (Barnard, 1964; Kilburn & Rippey, 1982). The latter species has been reported from Melkbos and False Bay indicating that its distribution is likely to be ubiquitous between these two localities and therefore present at Clifton (Iziko Marine Invertebrate Collections Database accessed 23/03/2021; SAMC-A056042 and SAMC-A029673).

Conclusion

While colonization of the wreck artefacts may not be ideal for maintaining the pristine nature of the biodiversity of the surrounding sandy bottom it presents both positive and negative consequences for the wreck itself. Layers of encrusting organisms, together with sediment, form concretion around the components of the wreck. This concretion may shield the artefacts from the degrading effects of the surrounding environment and thereby effectively preserves them. To date there is preliminary evidence that animals may be boring into the wooden structures of the *São José.* Establishing validated baseline information about the organisms inhabiting the *São José* and the surrounding environment, through dedicated sampling and expert identification, will be the first essential step towards understanding these fascinating interactions and position us to use this knowledge to inform future heritage and biodiversity management efforts.

References

Barnard, K. H. 1964. Contributions to the knowledge of South African marine mollusca. Part V. Lamellibranchiata. *Annals of the South African Museum*. **47**(3): 361-593

Bethencourt, M., Fernández-Montblanc, T., Izquierdo, A., González-Duarte, M.M. and Muñoz-Mas, C. 2018. Study of the influence of physical, chemical and biological conditions that influence the deterioration and protection of Underwater Cultural Heritage. *Science of the Total Environment*. **613**, pp.98-114.

Caporaso, A., Warren, D.J. and Gittings, S.R. 2018. The Evolution of Recent Multidisciplinary Deep-Water Archaeological and Biological Research on the Gulf of Mexico Outer Continental Shelf. In Historical Archaeology and Environment (pp. 207-226). Springer, Cham.

Hamdan, L.J., Salerno, J.L., Reed, A., Joye, S.B. and Damour, M. 2018. The impact of the Deepwater Horizon blowout on historic shipwreck-associated sediment microbiomes in the northern Gulf of Mexico. *Scientific reports*, **8**(1), p.9057.

Kilburn, R.N. & Rippey, E. 1982. Sea Shells of Southern Africa. Macmillan South Africa, Johannesburg, xi + 249 pp. page(s): 205

Meyer, K.S., Brooke, S.D., Sweetman, A.K., Wolf, M and Young, C.M. 2017. Invertebrates communities on historical shipwrecks in the western Atlantic: relation for. *Marine Ecology Progress series*. **566**:17-29.

CONCLUSION

We learnt many lessons during the development of the baseline environmental monitoring process. The importance of the data collected cannot be emphasized enough. We now have a better idea of the environment the wreck of the *São José* and can make informed decisions on whether it is best to attempt a complete excavation, partial excavation or implement total in situ conservation. One major outstanding dataset is the determination of the complete extents of the wreck site. As archaeological excavation was not a major objective of this study it follows that the data gathered will inform future archaeological work in order to establish the site extents.

One of the lessons learnt during the baseline study was not too rely too much on consultants. If one does use consultants it is important to make sure that deliverables are clear and well understood by all parties. Timelines are also important to establish although this is often constrained by uncontrollable factors such as the weather.

What is a more workable scenario is to have a dedicated team with specialized knowledge. It would have been better for example if the project employed an environmental scientist, maybe a student busy with an advanced degree, rather than a paid consultant. Consultants are more about business than development of new strategies as was the case in this project. If consultants are used it should be for specific discreet collection and interpretation of data. An example of this that worked extremely well during this project was the contracting of the Council for Geoscience for the multi beam sonar survey. They provided excellent and important data for the project and even did a second survey free of charge.

Suggested Methodology

To understand a dynamic environment such as a shipwreck site it is important to monitor it over a long period of time. So the first determination that has to be made is to establish the time period for the monitoring process. If a dedicated team with all the expertise needed is available this could be as little as three years. If external consultants are to be used it is better to extend this time period to five years.

The suggested disciplines involved in creating a baseline study are as follows:

1. Archaeology
2. Waterlogged objects Conservator
3. Marine Geophysics
4. Marine Biology
5. Oceanography

These five areas cover most of the needed monitoring specialties needed to obtain enough data to understand the environment around shipwreck sites.

Instrumentation needed for such a baseline monitoring project include the following:

1. Differential GPS – to measure beach sand levels
2. Multi-beam sonar – to measure bathymetry and sediment movement underwater

3. Dissolved Oxygen sensors to determine oxygen levels that helps inform conservation decisions
4. Conductivity sensors help determine rate of corrosion
5. Acoustic Current Doppler Profiler to determine wave action and current movement
6. Light sensors to determine biota growth zones

What we found during the *São José* study was that it was better to have your own sensors rather than hiring especially since weather patterns plays such a big role in when one can deploy sensors and when the sensors can be recovered. It is also important to have redundancy built in as sensors can be faulty. As such we purchased through the project dissolved oxygen, light and conductivity sensors. Iziko provided out of its own budget the purchase of Differential GPS equipment and an acoustic current Doppler profiler. This will enable us to continue collecting data not only on the *São José*, but also any new wreck site we would want to excavate in future.

The *São José* site

One of the main conclusions from the environmental monitoring project was that we should monitor for a longer period. Sensors should be deployed for at least a year and ideally quarterly or at least twice yearly multi beam surveys should be conducted. The reason we did not follow this strategy was that the funding did not allow for such an extensive data gathering. The multi beam sonar surveys especially are expensive and the only way forward would be a partnership with for example the Council for Marine Geoscience. Iziko also purchased its own acoustic current Doppler profiler just before the pandemic. Previously we hired this instrument for two periods of deployment as that was what the funding allowed. With our instrument we look forward to a longer term deployment.

We have determined with this study that the Clifton area and especially the site of the wreck of the *São José*, is exposed to violent forces of nature. The sediment movement during different seasons have a huge impact on which part of the wreck is exposed. Currents and wave action cause abrasion and dispersion of artefacts. The site is in a zone of high oxygen content which has mostly a negative effect on survival rate of artefacts. The highly dispersed nature of artefacts found so far indicates that there is more of the site to be found and explored. Now that we have data on the sand and water movement we can extrapolate that major parts of the wreck could lie towards the North West of the known artefacts possibly even under sand in the inter tidal zone.

We therefore recommend that any artefacts exposed should be recovered as there is a high likelihood that it will not survive exposure. The artefacts that should be left in situ are the three guns that remain a beacon of the site underwater and a large timber beam which may or may not relate to the shipwreck. The guns could be better protected for the long term by attaching sacrificial anodes to help counter corrosion.